50 kDa isoform contains only a six amino acid sequence in its N-terminal portion, which is apparently too short to interact with other molecules [10].

In this study, we overexpressed these recombinant proteins tagged with green fluorescent proteins (GFP) in CHO-IR cells and investigated intracellular localizations in the presence and absence of insulin stimulation. Only p85α and p85β redistributed to discrete foci in CHO-IR cells, while other isoforms did not. A recent study also demonstrated that GFP-p85α translocates to similar foci in CHO-K1 cells in response to insulin-like growth factor-1 (IGF-1) stimulation [11]. We have demonstrated these isolated foci to be composed of p85 and IRS-1 by immunohistochemistry and western blotting using an immunoprecipitation method, and found the SH3 domain located in the N-terminal portion of p85 to be responsible for the formation of foci with IRS-1. As monomeric p85 was previously demonstrated to down-regulate insulin signaling by competing with the p85-p110 dimer for IRS-1 binding [12], the formation of p85-IRS-1 foci is likely to be involved in the mechanism of negative regulation of insulin signaling.

Materials and methods

cDNA constructs of each PI 3-kinase regulatory subunit isoform. Rat cDNAs encoding the full-length amino acid sequences of p85α, p85β, p55α, p55γ, and p50α [13], as well as the GFP cDNA (CLONTECH, Laboratories, Inc.) at each N-terminus, were ligated into the EcoRI sites of pSRα vectors. cDNA of the SH3 domain deletion mutant (SH3D) of p85α was prepared as previously described by PCR methods [14] and similarly inserted into pSRα vectors. Fragments prepared by PCR were fully sequenced and observed to have no unexpected mutations.

Cell culture and transfections. CHO-IR cells were maintained in DMEM with 4500 mg/L glucose, containing 10% fetal calf serum (Life Technologies, Inc.) at 37 °C in 5% CO_2. Lipofectamine reagent, Opti-MEM I, was purchased from Gibco-BRL Life Technologies (Eggenstein, Germany). One day before transfection, CHO-IR cells were trypsinized and seeded onto a 60-mm plastic culture dish at 6×10^5 cells/dish. The following day, the transfection procedures were performed using 30 μl of lipofectamine diluted in 300 μl of Opti-MEM I and 6 μg of plasmid DNA diluted in 300 μl of supplemental Opti-MEM-I per 60-mm dish. Cells were incubated in the presence of the lipofectamine-DNA mix for 5 h at 37 °C, in 5% CO_2, and then incubated overnight in DMEM-10% FCS. Forty-eight hours after transfection, each transfected 60-mm dish was used for experiments.

Antibodies and Western blotting. Western blotting was performed as previously described [15]. Commercial antibodies against murine GFP (Chemicon International, CA), phospho-Akt (Ser 473) (Cell Signaling Technology, CA), phophotyrosine, 4G10 (Upstate Biotechnology, NY), and IRS-1 (Cell Signaling Technology, CA) were purchased. After blotting with the indicated secondary antibody, detection was performed using an ECL chemiluminescent kit (Amersham Pharmacia Biotech, UK). Quantitations were performed using a Molecular Imager (Bio-Rad Lab, CA). Immunoprecipitation was performed as previously described [16], using anti-IRS-1 and GFP antibodies. Immunoprecipitates were then boiled in Laemmli sample buffer, subjected to SDS–PAGE, and finally to Western blotting using the anti-phosphotyrosine (4G10) or GFP antibodies.

Immunofluorescence analysis. Immunofluorescence studies were performed as previously described [15]. Cells were plated at near-confluent density on glass coverslips and fixed in 4% paraformaldehyde–PBS for 20 min at room temperature. Coverslips were washed three times in PBS, then quenched for 15 min in 0.2% Triton X-100. After a further three washes in PBS, coverslips were blocked for 30 min in 2% horse serum-PBS and then washed twice in PBS. Commercial primary antibodies against IRS-1 (Cell Signaling Technology, CA), insulin receptor (Santa Cruz Biotechnology, Germany), Caveolin (BD Biosciences, CA), and p110α [17] were used. These antibodies were diluted in 0.1% horse serum-PBS, and incubations were carried out at 4 °C overnight. Tetramethyl rhodamine isothiocyanate (TRITC)-conjugated anti-mouse immunoglobulin secondary antibody (Zymed Lab., CA) diluted in 0.1% horse serum–PBS was applied after three 5 min washes in PBS. After 1 h of incubation, at RT, coverslips were washed three times in PBS for 5 min each and then mounted in 1% propyl gallate–50% glycerol–PBS and finally observed under a microscope.

Method of delivering peptides into CHO-IR cells. We delivered peptides into CHO cells using Chariot Transfection Reagent (Active Motif, CA). Briefly, 6 μl of Chariot were diluted in 60% DMSO up to 100 and 100 μl of PBS were added to 50 μg of synthesized proline-rich peptides (PRM1, PPTPKPRPPRPLPVAP). The 100 μl proline dilution was added to the 100 μl Chariot dilution, followed by incubation at RT for 60 min to allow the Chariot-proline complex to form. The cells to be transfected in a six-well tissue culture plate were overlaid with the 200 μl Chariot-proline complex, followed by addition of 400 μl of serum-free medium and incubation for 1hr. Then, we added 1 ml of complete growth medium to the cells and continued the incubation for 1 h. Next, we aspirated the complete growth medium, washed twice with 2 ml of PBS, added serum free medium containing 0.2% BSA and incubated the cells at 37 °C in 5% CO2 for 5 h. After incubation with or without 100 nM insulin for 10 min and washing once with PBS, the cells were fixed with 4% paraformaldehyde for 10 min. After washing with PBS, the cells were observed by fluorescence microscopy. Positive control peptides, 2 μg of β-galactosidase, were transfected into the cells using the same techniques, except for β-galactosidase staining, achieved using a β-galactosidase staining kit (Active Motif, CA).

Results

The schematic structures of five wild-type and one SH3 deletion mutant regulatory subunit isoform of PI 3-kinase are shown in Supplementary Fig. 1. First, we overexpressed wild-type recombinant proteins tagged with GFP in CHO-IR cells and investigated intracellular localizations in both the presence and the absence of insulin stimulation (Fig. 1). Control GFP were found to exhibit intracellular localizations with a greater preference for the nucleus. Interestingly, in contrast to control GFP, p85α, and p85β redistributed to discrete foci in the cells in response to insulin, while they were seen throughout the cytoplasm in quiescent cells. Other isoforms showed no changes in localization with insulin stimulation. The p55α and p55γ exhibited concentrated accumulations around the perinuclear region. In particular, p55γ was restricted to the perinuclear region, while p55α was also distributed throughout the cytoplasm. On the other hand, the distribution of p50α was very similar to that of control GFP.

To investigate the properties of these isolated foci, we searched for proteins co-localized with overexpressed p85-GFP proteins. First, we performed immunofluorescence analyses using antibodies against the insulin receptor, caveolin and the catalytic subunit of PI 3-kinase, p110α, as primary antibodies. However, the signals obtained from these studies were not associated with the foci observed in the cytoplasm when p85α-GFP proteins were overex-

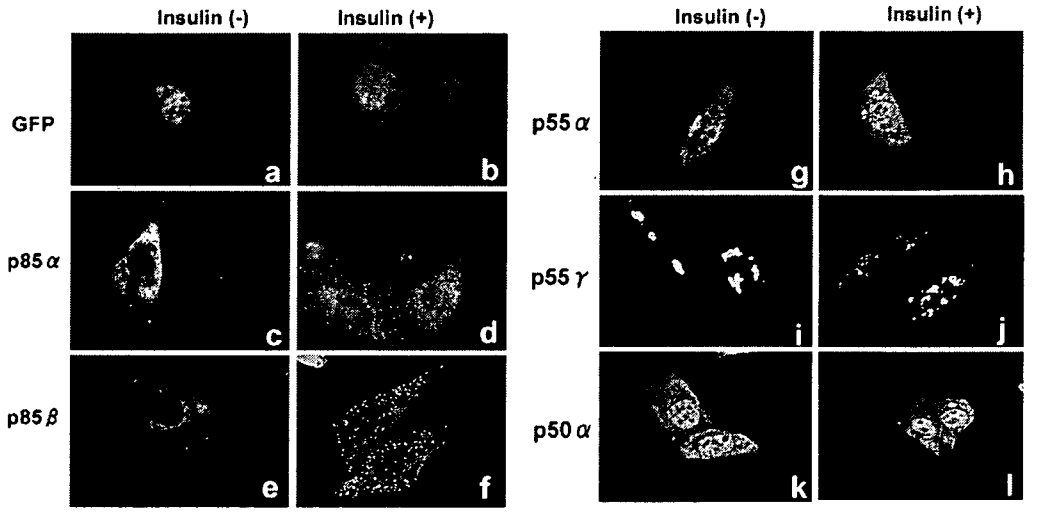

Fig. 1. The localizations of each PI 3-kinase regulatory subunit-GFP protein in CHO-IR cells in the absence and presence of insulin. CHO-IR cells were seeded onto a 60-mm plastic culture dish at 6×10^5 cells/dish. The following day, transfection procedures were performed using 30 μl of lipofectamine diluted in 300 μl of Opti-MEM I and 6 μg of pSRα vector DNA containing cDNA of GFP (a,b), p85α-GFP (c,d), p85β-GFP (e,f), p55α-GFP (g,h), p55γ-GFP (i,j), and p50α-GFP (k,l). Cells were incubated in the presence of the lipofectamine-DNA mix for 5 h, and then incubated overnight in DMEM containing 10% FCS. Forty-eight hours after transfection, each of the transfected 60-mm dishes was used for experiments. Before the experiments, CHO-IR cells were serum starved and stimulated with insulin for 10 min (b, d, f, h, j, and l). The results shown are representative of three experiments.

pressed (data not shown). Interestingly, only the signals observed in an immunofluorescence study using antibodies against IRS-1 corresponded to with these foci (Fig. 2h), suggesting that IRS-1 co-localized with these p85 foci in response to insulin. Though we cannot rule out the possibility that the p85-IRS-1 complex contains other unex-

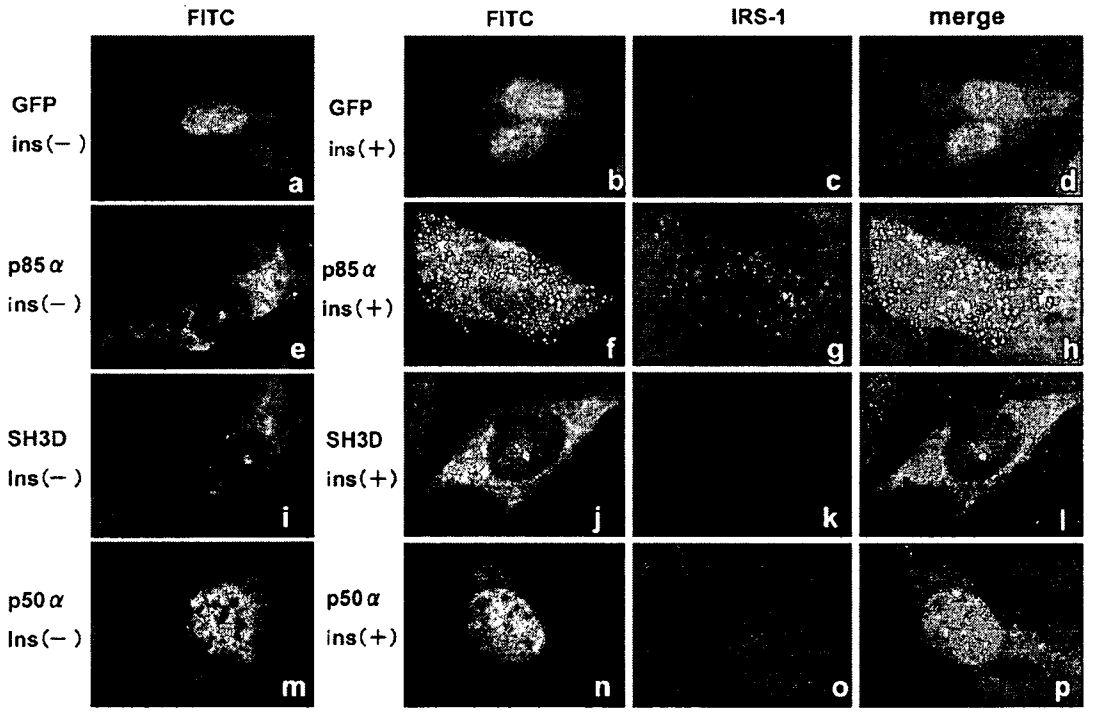

Fig. 2. Immunofluorescence analyses of PI 3-kinase regulatory subunit-GFP proteins. CHO-IR cells were plated at near-confluent density and were transfected with GFP (a–d), p85α-GFP (e–h), SH3D-GFP (i–l) or p50α-GFP(m–p). Cells were serum starved and stimulated with insulin for 10 min. Cells were fixed in 4% paraformaldehyde–PBS for 20 min, then quenched for 15 min in 0.2% Triton X-100. Commercial primary antibodies against IRS-1 were diluted in 0.1% horse serum–PBS, and incubations were carried out at 4 °C overnight. TRITC-conjugated anti-mouse immunoglobulin secondary antibody diluted in 0.1% horse serum-PBS was applied after three 5 min washes in PBS. After a 1 h incubation, coverslips were mounted in 1% propyl gallate–50% glycerol–PBS and were observed under a microscope. Results shown are representative of three experiments.

pected proteins, both the insulin receptor and p110α catalytic subunits are absent from these foci according to immunofluorescence results, suggesting that only p85 and the IRS-1 dimer form a sequestration complex in response to insulin. As p55s and p50α did not form foci, we expected that the domain responsible for IRS-1 complex formation would be either the SH3 domain or the bcr homology (BH) domain. Thus, we prepared and overexpressed the SH3 domain deletion mutant (SH3D) of p85α-GFP in CHO-IR cells. This mutant failed to form foci (Fig. 2j), i.e., the SH3 domain of regulatory subunits is likely to be responsible for formation of the p85-IRS-1 sequestration complex. Based on a previous report that SH3 domain-proline rich motif inertactions mediate dimerization of PI-3 kinase regulatory subunits [18], we examined whether these interactions are involved in formation of the sequestration complex with IRS-1. After confirming that β-galactosidase, as a positive control peptide, was properly transfected in our experiments (Supplementary Fig. 2a), proline-rich motif peptides were similarly transfected into CHO-IR cells. As shown in Supplementary Fig. 2e, proline-rich peptides did not affect p85-IRS-1 complex formation, indicating that SH3-domain-proline-rich motif interactions are unlikely to be involved in this complex formation.

Though p85α-IRS-1 complexes formed in response to insulin stimulation, as demonstrated by immunofluorescence analysis, we attempted to further demonstrate these direct associations by immmunoprecipitation. After confirming that almost equal amounts of p85α, SH3D, and p50α-GHP proteins had been expressed in CHO-IR cells (Fig. 3, upper panel), we performed immunoprecipitation experiments using either anti-IRS-1 or anti-GFP antibody and blotted the transferred sheets with anti-GFP or anti-phopho-tyrosine antibody (4G10), respectively. As expected, an insulin-dependent IRS-1 association with p85α-GFP was detected (Fig. 3, middle and lower panels). Despite the lack of IRS-1 complex formation, IRS-1 associations with both the SH3D mutant and p50α-GFP were also observed. Moreover, only IRS-1-SH3D mutant binding was present in the absence of insulin stimulation. Thus, even though the overexpressed regulatory subunits fail to form discrete foci, these subunits do actually bind to IRS-1 in the presence of insulin.

Next, we investigated downward signaling by analyzing Ser473-Akt phosphorylation in the presence of insulin with overexpression of each isoform. As shown in Fig. 4, p85α and SH3D mutant-GFP overexpressions markedly diminished insulin dependent Akt phosphorylations, while p50α-GFP overexpression did not affect Akt phosphorylation as compared with control cells. Based on a previous report demonstrating monomeric p85 to down-regulate insulin signaling by competing with the p85-p110 dimer for IRS-1 binding [12], p85α-GFP and the SH3D mutant also negatively suppressed insulin signaling by removing IRS-1 from p85-p110-IRS trimers.

Discussion

In this study, we overexpressed five class IA PI 3-kinase regulatory subunit isoforms tagged with GFP in CHO-IR cells and investigated intracellular localizations in response to insulin stimulation. p85α and p85β redistributed to discrete foci in CHO-IR cells, while other isoforms did not. p55α and p55γ preferentially remained in the perinuclear

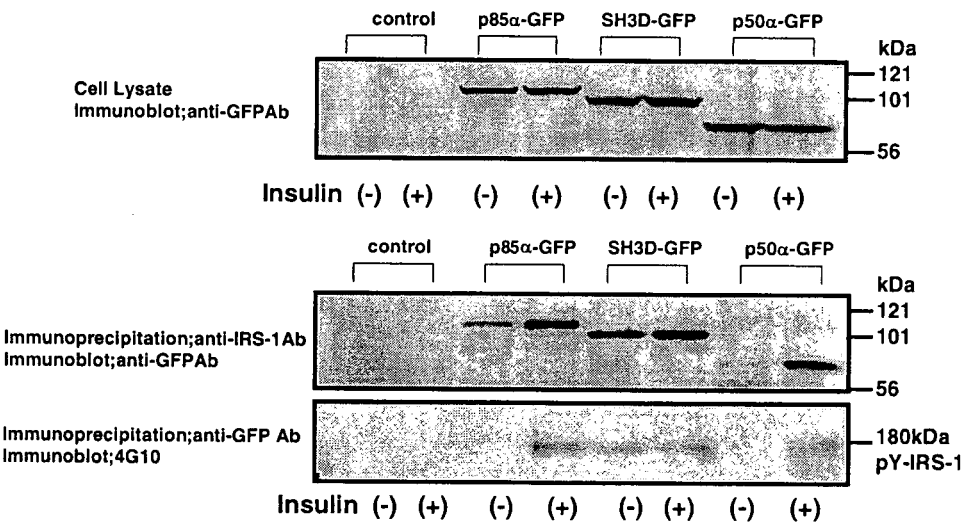

Fig. 3. Direct associations between IRS-1 proteins and each PI 3-kinase regulatory subunit isoform. CHO-IR cells were transfected with only the pSRα vector, pSRα DNA containing cDNA of p85α-GFP, SH3D-GFP, or p50α-GFP. After serum starvation, cells were stimulated with insulin for 10 min. Supernatants including tissue protein extracts were resolved on 10% SDS–polyacrylamide gel, followed by electrophoretic transfer to a nitrocellulose membrane. Membranes were incubated for 1 h at RT with anti-GFP antibody. After blotting with anti-GFP antibody, detection was performed using an ECL chemiluminescence kit (upper panel). Immunoprecipitation was performed using anti-IRS-1 (middle panel) and GFP antibodies (lower panel). Immunoprecipitates were then boiled in Laemmli sample buffer, subjected to SDS–PAGE, and finally to Western blotting using anti-GFP (middle panel) and anti-phosphotyrosine antibodies (lower panel). Three independent experiments were performed and similar results were obtained.

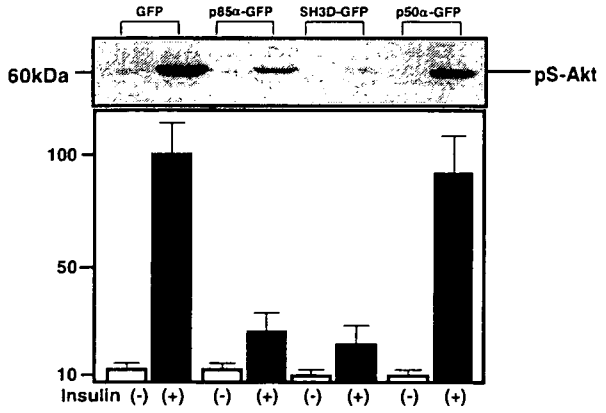

Fig. 4. Effects of overexpressing each isoform of the PI 3-kinase regulatory subunit on Ser473-Akt phosphorylation in CHO-IR cells. CHO-IR cells were transfected with only pSRα vector, pSRα DNA containing cDNA of p85α-GFP, SH3D-GFP or p50α-GFP. After serum starvation, cells were stimulated with insulin for 10 min. Supernatants including tissue protein extracts were resolved on 10% SDS–polyacrylamide gel, followed by electrophoretic transfer to a nitrocellulose membrane. Membranes were incubated for 1 h at RT with anti-phospho-Akt (Ser473) antibody. After blotting with the indicated secondary antibody, detection was performed using an ECL chemiluminescent kit. Quantitations were performed using a Molecular Imager. Three independent experiments were performed and similar results were obtained.

region, while p50α exhibited localizations very similar to that of the control GFP. The signal sequence of p55s is located in the N-terminal domain, which is composed of a unique 34 amino-acid sequence. It was previously reported that this 34 amino-acid sequence has a high affinity for α/β tubulin [19] or the retinoblastoma tumor suppressor protein (Rb), a key regulator of cell cycle progression [20]. Further study is needed to investigate whether perinuclear localizations are related to the associations with these proteins.

Though PI 3-kinase plays a key role in mediating insulin signals downstream from IRS-1, mice lacking the p85α or p85β subunits of PI 3-kinase, paradoxically, show high insulin sensitivity [21,22]. There are two possible explanations for this discrepancy. First, p50α subunits were previously demonstrated to exhibit a markedly higher capacity for activation of associated PI 3-kinase via insulin stimulation and to have a higher affinity for tyrosine-phosphorylated IRS-1 than other isoforms [10]. In mice lacking p85s, there are more p50α subunits and they substitute for the missing p85s subunits [21,22], thereby producing enhanced insulin sensitivity. In fact, the overexpression of p50α-GFP also resulted in high insulin sensitivity being maintained in this study. Second, p85s regulatory subunits have two SH2 domains separated by an inter-SH2 domain, through which they bind p110 catalytic subunits, and in addition, monomeric p85s and p85s–p110s mutually compete for IRS-1 binding [12]. Thus, the molecular balance between p85s and p110s might have a major effect on insulin signaling downstream from PI 3-kinase. We can speculate that fewer p85s subunits means greater insulin sensitivity. Inversely, if an excess of monomeric p85s is present, insulin signaling might be inhibited by p85s-IRS-1 dimers, which have no ability to transmit insulin signals, and thus serve as a dominant negative form.

Subsequently, it was clearly demonstrated that p85α-IRS-1 dimers form a sequestration complex in response to IGF-1 stimulation [11]. We observed similar p85-IRS-1 complexes in the case of insulin stimulation in p85s-GFP transfected CHO-IR cells and showed the p85α-SH3 domain to be responsible for complex formation. Based on a previous report describing the isolated p85α-SH3 domain as binding only one of its endogenous proline-rich motifs, PRM1 (Fig. 1) [18], we examined whether SH3-PRM1 interactions are involved in forming the sequestration complex with IRS-1. However, PRM1 peptides were incapable of disrupting the p85α-IRS-1 complex, suggesting that other interactions with the SH3 domain, such as the SH3-BH domain [23], might be involved in this complex formation.

In conclusion, when five PI 3-kinase regulatory subunit isoforms tagged in their C-terminal tails with GFP were overexpressed in CHO-IR cells, only p85α and p85β redistributed to discrete foci in response to insulin. We immunohistochemically demonstrated that these isolated foci are composed of p85 and IRS-1 and found the SH3 domain located in the N-terminal portion of p85 to be responsible for the formation of foci with IRS-1. These p85-IRS-1 complex formations represent negative regulation of insulin signaling due to a molecular imbalance between p85s and p110s.

Appendix A. Supplementary data

Supplementary data associated with this article can be found, in the online version, at doi:10.1016/j.bbrc.2007.10.187.

References

[1] B. Cheatham, C.J. Vlahos, L. Cheatham, L. Wang, J. Blenis, C.R. Kahn, Phosphatidylinositol 3-kinase is required for insulin stimulation of pp70 S6 kinase, DNA synthesis, and glucose transporter translocation, Mol. Cell. Biol. 14 (1994) 4902–4911.

[2] K. Kimura, S. Hattori, Y. Kabuyama, Y. Shizawa, J. Takayanagi, S. Nakamura, S. Toki, Y. Matsuda, K. Onodera, Y. Fukui, Neurite outgrowth of PC12 cells is suppressed by wortmannin, a specific inhibitor of phosphatidylinositol 3-kinase, J. Biol. Chem. 269 (1994) 18961–18967.

[3] S. Wennstrom, P. Hawkins, F. Cooke, K. Hara, K. Yonezawa, M. Kasuga, T. Jackson, L. Claesson-Welsh, L. Stephens, Activation of phosphoinositide 3-kinase is required for PDGF-stimulated membrane ruffling, Curr. Biol. 4 (1994) 385–393.

[4] R. Yao, G.M. Cooper, Requirement for phosphatidylinositol-3 kinase in the prevention of apoptosis by nerve growth factor, Science 267 (1995) 2003–2006.

[5] H. Katagiri, T. Asano, H. Ishihara, K. Inukai, Y. Shibasaki, M. Kikuchi, Y. Yazaki, Y. Oka, Overexpression of catalytic subunit p110alpha of phosphatidylinositol 3-kinase increases glucose transport activity with translocation of glucose transporters in 3T3-L1 adipocytes, J. Biol. Chem. 271 (1996) 16987–16990.

[6] D.J.V. Horn, M.G. Myers Jr., J.M. Backer, Direct activation of the phosphatidylinositol 3′-kinase by the insulin receptor, J. Biol. Chem. 269 (1994) 29–32.
[7] P. Hu, A. Mondino, E.Y. Skolnik, J. Schlessinger, Cloning of a novel, ubiquitously expressed human phosphatidylinositol 3-kinase and identification of its binding site on p85, Mol. Cell. Biol. 13 (1993) 7677–7688.
[8] S. Pons, T. Asano, E. Glasheen, M. Miralpeix, Y. Zhang, T.L. Fisher, M.G. Myers, X.J. Sun, M.F. White, The structure and function of p55PIK reveal a new regulatory subunit for phosphatidylinositol 3-kinase, Mol. Cell. Biol. 15 (1995) 4454–4465.
[9] K. Inukai, M. Anai, E.V. Breda, T. Hosaka, H. Katagiri, M. Funaki, Y. Fukushima, T. Ogihara, Y. Yazaki, M. Kikuchi, Y. Oka, T. Asano, A novel 55-kDa regulatory subunit for phosphatidylinositol 3-kinase structurally similar to p55PIK Is generated by alternative splicing of the p85α gene, J. Biol. Chem. 271 (1996) 5317–5320.
[10] K. Inukai, M. Funaki, T. Ogihara, H. Katagiri, A. Kanda, M. Anai, Y. Fukushima, T. Hosaka, M. Suzuki, B.S. Shin, K. Takata, Y. Yazaki, M. Kikuchi, Y. Oka, T. Asano, p85α gene generates three isoforms of regulatory subunit for phosphatidylinositol 3-kinase (PI 3-Kinase), p50α, p55α, and p85α, with different PI 3-kinase activity elevating responses to insulin, J. Biol. Chem. 272 (1997) 7873–7882.
[11] J. Luo, S.J. Field, J.Y. Lee, J.A. Engelman, L.C. Cantley, The p85 regulatory subunit of phosphoinositide 3-kinase down-regulates IRS-1 signaling via the formation of a sequestration complex, J. Cell Biol. 170 (2005) 455–464.
[12] K. Ueki, P. Algenstaedt, F. Mauvais-Jarvis, C.R. Kahn, Positive and negative regulation of phosphoinositide 3-kinase dependent signaling pathways by three different gene products of the p85 α regulatory subunit, Mol. Cell. Biol. 20 (2000) 8035–8046.
[13] K. Inukai, M. Funaki, M. Anai, T. Ogihara, H. Katagiri, Y. Fukushima, H. Sakoda, Y. Onishi, H. Ono, M. Fujishiro, M. Abe, Y. Oka, M. Kikuchi, T. Asano, Five isoforms of the phosphatidylinositol 3-kinase regulatory subunit exhibit different associations with receptor tyrosine kinase and their tyrosine phosphorylations, FEBS Lett. 490 (2001) 32–38.
[14] K. Inukai, A.M. Shewan, W.S. Pascow, S. Katayama, D.E. James, Y. Oka, Carboxy terminus of glucose transporter 3 contains an apical targeting domain, Mol. Endocrinol. 18 (2004) 339–349.
[15] K. Inukai, M. Watanabe, Y. Nakashima, N. Takata, A. Isoyama, T. Sawa, S. Kurihara, T. Awata, S. Katayama, Glimepiride enhances intrinsic peroxisome proliferator-activated receptor-gamma activity in 3T3-L1 adipocytes, Biochem. Biophys. Res. Commun. 328 (2005) 484–490.
[16] K. Imai, K. Inukai, Y. Ikegami, T. Awata, S. Katayama, LKB1, an upstream AMPK kinase, regulates glucose and lipid metabolism in cultured liver and muscle cells, Biochem. Biophys. Res. Commun. 351 (2006) 595–601.
[17] M. Funaki, H. Katagiri, A. Kanda, M. Anai, M. Nawano, T. Ogihara, K. Inukai, Y. Fukushima, H. Ono, Y. Yazaki, M. Kikuchi, Y. Oka, T. Asano, p85/p110-type phosphatidylinositol kinase phosphorylates not only the D-3, but also the D-4 position of the inositol ring, J. Biol. Chem. 274 (1999) 22019–22024.
[18] A.G. Harpur, M.J. Layton, P. Das, M.J. Bottomley, G. Panayotou, P.C. Driscoll, M.D. Waterfield, Intermolecular interactions of p85α regulatory subunit of phosphoatidylinositol 3-kinase, J. Biol. Chem. 274 (1999) 12323–12332.
[19] K. Inukai, M. Funaki, M. Nawano, H. Katagiri, T. Ogihara, M. Anai, Y. Onishi, H. Sakoda, H. Ono, Y. Fukushima, M. Kikuchi, Y. Oka, T. Asano, The N-terminal 34 residues of the 55 kDa regulatory subunits of phosphoinositide 3-kinase interact with tubulin, Biochem. J. 346 (2000) 483–489.
[20] X. Xia, A. Cheng, D. Akinmade, A.W. Hamburger, The N-terminal 24 amino acids of the p55g regulatory subunit of phosphoinositide 3-kinase binds Rb and induce cell cycle arrest, Mol. Cell. Biol. 23 (2003) 1717–1725.
[21] Y. Terauchi, Y. Tsuji, S. Satoh, H. Minoura, K. Murakami, A. Okuno, K. Inukai, T. Asano, Y. Kaburagi, K. Ueki, H. Nakajima, T. Hanafusa, Y. Matsuzawa, H. Sekihara, Y. Yin, J.C. Barrett, H. Oda, T. Ishikawa, Y. Akanuma, I. Komuro, M. Suzuki, K. Yamamura, T. Kodama, H. Suzuki, T. Kadowaki, Increased insulin sensitivity and hypoglycemia in mice lacking the p85α subunit of phosphatidylinositide 3-kinase, Nat. Genet. 21 (1999) 230–235.
[22] K. Ueki, C.M. Yballe, S.M. Brachmann, D. Vicent, J.M. Watt, C.R. Kahn, L.C. Cantley, Increased insulin sensitivity in mice lacking p85β subunit of phosphoinositide 3-kinase, Proc. Natl. Acad. Sci. USA 99 (2002) 419–424.
[23] A. Musacchio, L.C. Cantley, S.C. Harrison, Crystal structure of the breakpoint cluster region-homology domain from phosphoinositide 3-kinase p85 α subunit, Proc. Natl. Acad. Sci. USA 93 (1996) 14373–14378.

DIABETES RESEARCH AND CLINICAL PRACTICE 79 (2008) 2–10

available at www.sciencedirect.com

ScienceDirect

journal homepage: www.elsevier.com/locate/diabres

Regulation of gut-derived resistin-like molecule β expression by nutrients

Junko Fujio [a,b], *Akifumi Kushiyama* [b], *Hideyuki Sakoda* [b], *Midori Fujishiro* [b], *Takehide Ogihara* [c], *Yasushi Fukushima* [a], *Motonobu Anai* [d], *Nanao Horike* [a], *Hideaki Kamata* [e], *Yasunobu Uchijima* [a], *Hiroki Kurihara* [a], *Tomoichiro Asano* [a,e,*]

[a] *Department of Physiological Chemistry and Metabolism, Graduate School of Medicine, University of Tokyo, 7-3-1 Hongo, Bunkyo-ku, Tokyo 113-0033, Japan*

[b] *Department of Internal Medicine, Graduate School of Medicine, University of Tokyo, 7-3-1 Hongo, Bunkyo-ku, Tokyo 113-0033, Japan*

[c] *Division of Advanced Therapeutics for Metabolic Diseases, Center for Translational and Advanced Animal Research on Human Diseases, Tohoku University Graduate School of Medicine, 2-1 Seiryo-machi, Sendai, Japan*

[d] *Institute for Adult Diseases, Asahi Life Foundation, 1-6-1 Marunouchi, Chiyoda-ku, Tokyo 100-0005, Japan*

[e] *Department of Medical Science, Graduate School of Medicine, University of Hiroshima, 1-2-3 Kasumi, Minami-ku, Hiroshima City, Hiroshima 734-8551, Japan*

ARTICLE INFO

Article history:
Received 25 August 2006
Received in revised form
19 February 2007
Accepted 16 April 2007
Published on line 23 October 2007

Keywords:
RELMβ
Nutrient compositions
Insulin resistance

ABSTRACT

Resistin was initially identified as a protein, secreted by adipocytes, which inhibits insulin action and adipose differentiation. The three proteins homologous to resistin were identified and given the names resistin-like molecules (RELM) α, β and γ. Resistin and RELMα are abundantly expressed in adipose, but RELMβ and RELMγ are secreted mainly from the gut. Since nutrient composition greatly affects insulin sensitivity, we investigated the regulatory effects of various nutritional factors in food on the expressions of resistin family proteins.

First, mice were given diets with different nutritional compositions (high-carbohydrate, high-protein and high-fat) for 2 weeks. RELMβ mRNA expression in the intestines was markedly suppressed by the high-protein and high-carbohydrate diets, while slightly but not significantly upregulated by the high-fat diet. In the epididymal fat, resistin expression was unchanged, while RELMα expression was markedly decreased by the high-carbohydrate diet. Taking into consideration that humans have neither RELMα nor RELMγ, our subsequent studies focused on RELMβ expression. We used the human colon cancer cell line LS174T. Treatments with insulin and TNFα as well as stearic acid, a saturated free fatty acid, upregulated RELMβ expression, while D-glucose downregulated RELMβ. These results suggest RELMβ expression to be regulated directly by nutrients such as glucose and saturated free fatty acids including stearic acid, as well as by hormones including insulin and TNFα. These regulations may play an important role in the nutrient-associated induction of insulin resistance.

* *Corresponding author.* Tel.: +81 82 257 5135; fax: +81 82 257 5136.
E-mail address: asano-tky@umin.ac.jp (T. Asano).

0168-8227/$ – see front matter © 2007 Elsevier Ireland Ltd. All rights reserved.
doi:10.1016/j.diabres.2007.04.015

1. Introduction

Resistin and its related proteins, i.e. resistin-like molecules (RELMs) α, β and γ, are a family of recently identified proteins [1,2]. They share an N-terminal signal sequence and a C-terminal region with a unique structure that contains 10 cysteine residues [3]. Resistin was identified as an adipocyte secreted factor, expression of which is increased in genetically obese (*ob/ob* and *db/db*) mice [4]. Furthermore, administration of resistin reportedly impairs glucose tolerance and reduces insulin action in normal mice, both of which are reversed by immunoneutralization with anti-resistin antibody [4]. Resistin knock-out mice were also described as having lower fasting blood glucose [5]. However, there are conflicting observations regarding its function as a factor responsible for insulin resistance [6–9].

RELMα is a secreted protein of 111 amino acids that has been identified in rats and mice and is expressed in the lungs, white adipose tissue and the intestines. There is a difference between the two species in that RELMα expression in white adipose tissue is much lower in rats than in mice [2,3]. This protein has been shown to inhibit the differentiation of adipocytes *in vitro* [10]. RELMα is induced by Th2 type cytokines in rodent pulmonary epithelial cells, and thus is likely to be involved in the inflammatory response [11]. RELMγ was also initially identified in the nasal respiratory epithelium of rats [2], and was revealed to be expressed in bone marrow, peripheral blood granulocytes, the spleen, lungs and pancreas as well as the large and small intestines of mice [2,12,13].

RELMβ is highly expressed in goblet cells of the murine colon and secreted in response to bacterial colonization [14], and thus was suggested to play an important role in defense against nematode parasitization in mice [15]. On the other hand, we previously reported that RELMβ and RELMγ are present in blood, and that their serum concentrations and expressions in the colon were elevated in insulin resistant models such as obese *db/db* mice and high-fat-fed mice [16]. In addition, transgenic mice which overexpressed RELMβ in the liver, exhibited hyperglycemia, hyperlipidemia and fatty liver [17]. Thus, we consider intestine-derived RELMβ to be involved in insulin resistance.

The first objective of this study was to investigate the regulatory effects of nutritional factors in different diets on the expressions of resistin and RELMs. Interestingly, the expression of RELMβ, but not resistin, was found to be strongly influenced by different dietary compositions. Although there are four genes encoding this protein family in the mouse, only resistin and RELMβ have been identified in the human genome sequence [2]. Thus, we focused on the regulation of RELMβ expression, and performed additional experiments using cultured cells to examine whether nutritional factors, as well as hormones such as insulin and TNFα, are direct regulators of RELMβ expression. Herein, we show the regulation of gut-derived RELMβ to be regulated by both nutrients and hormones, and that its upregulation may be involved in the pathogenesis of diet-derived insulin resistance.

2. Materials and methods

2.1. Reagents and antibodies

All reagents were of analytical grade and anti-RELMβ antibody was purified as previously described [17].

2.2. Animal studies

Six-week-old mice (C57BL/6J) were purchased from CLEA Inc and housed under conventional conditions. All animal studies were performed after 2–3 days acclimation period and mice were anesthetized with pentobarbital. To determine RELMβ expression levels in fed and fasted states, the colon was excised from both mice fed *ad libitum* and those fasted for 18 h ($n = 3$ per group). In the fasted state, both the colon and the ileum were collected to assess the correlation between RELMβ mRNA levels in these tissues ($n = 22$). In the dietary studies, animals were divided into four groups receiving different diets, i.e. high-carbohydrate (CA), high-protein (P), high-fat (HF) and control (C) diets, and were fed *ad libitum* for 2 weeks ($n = 4$–5 per group) or fed once ($n = 6$ per group), to assess both acute and chronic effects of these diets. The compositions of the diets are shown in Table 1. With 2 week feeding, at the end of the 2-week period, the animals were fasted for 18 h. Then, blood, colon and epididymal fat, as a representative white adipose tissue, samples were collected. Tissue samples were homogenized in an adequate amount of ice-cold Isogen (Nippon Gene) directly for mRNA extraction or ice-cold Lysis Buffer (10 mM HEPES pH 7.4, 150 mM NaCl, 2 mM EDTA, 1% Triton-X 100, 2 mM PMSF, 2 μg/ml aprotinin, 5 μg/ml leupeptin) after careful removal of stool, for Western blotting. Serum was separated, after a sufficient time at room temperature to allow coagulation, by centrifugation at 3000 rpm for 20 min followed by 1 min at 15000 rpm. Lipid and other parameters were measured in the sera obtained.

Animal care and procedures for the experiments were performed according to the Japanese guidelines for the care and use of experimental animals.

Table 1 – Dietary compositions

	Control diet (3.58 Kcal/g)		High carbohydrate (3.55 kcal/g)		High protein diet (3.47 kcal/g)		High fat diet (6.66 kcal/g)	
	%weight	%kcal	%weight	%kcal	%weight	%kcal	%weight	%kcal
Protein	23.3	26	13	14	70	79.8	24.2	14.6
Fat	5.3	13.3	1	4.4	1	5.7	60	81
Carbohydrate	53.8	60.1	80	81.6	10	12.5	7.3	4.4

2.3. *Intraperitoneal glucose tolerance tests*

Glucose tolerance tests were performed after the 2-week feeding period. After an overnight fast, 2 g/kg D-glucose was injected intraperitoneally after the initial glucose measurement. Glucose levels were again determined at 15, 30, 60, 90 and 120 min after the injection. Glucose was measured by tail snipping. Three or four mice from each group were subjected to this test.

2.4. *Cell culture*

LS174T cells were obtained from the Cell Resource Center for Biomedical Research (Sendai, Japan), and cultured in RPMI 1640 (Sigma) medium supplemented with 10% FCS (Invitrogen), Penicillin 100 U/ml and Streptomycin 100 μg/ml (GIBCO Invitrogen) at 37 °C in 5% CO_2. Cells were cultured on 24 well plates (IWAKI) for the extraction of mRNA for stimulation tests. At 80% confluence, each well was washed twice with PBS and subsequently incubated under various conditions described below for 24 h, and the cells were then subjected to the mRNA extraction.

For insulin and TNFα stimulation, insulin and TNFα were added to RPMI 1640 to give final concentrations of 100 nM and 100 ng/ml, respectively. For glucose stimulation, RPMI 1640 supplemented with D-glucose to achieve final concentrations of 5, 11 or 25 mM was used and RPMI 1640 containing L-glucose at the same concentrations was used for the controls. Furthermore, linoleic acid (LA), oleic acid (OA) and stearic acid (SA) resolved in ethanol and conjugated with 20% bovine serum albumin (BSA) were added to RPMI 1640 to give two final concentrations, 0.5 and 2.0 mM, for each FFA. For control samples, medium adjusted only with ethanol and BSA was used.

2.5. *RNA isolation and quantification by real time quantitative polymerase chain reaction*

Total RNA was extracted from murine tissue samples, or cultured LS174T cells, using Isogen (Nippon Gene) according to the manufacturer's instructions. The cDNA was synthesized from total RNA using a First Strand cDNA Synthesis Kit for RT-PCR (Roche Diagnostics) according to the manufacturer's instructions. The oligonucleotide primers were designed using program Primer 3 (http://frodo.wi.mit.edu/cgi-bin/primer3/) and produced by Japan Bio Service, (Saitama, Japan). mRNA expressions for RELMs and resistin were quantified on a Light Cycler Instrument (Roche) using Light Cycler DNA Master SYBR Green I. The results were standardized against internal controls, m36B4 or h36B4 for the mouse tissue and LS174T cell-derived mRNA, respectively. The primer sequences used for human RELMβ (hRELMβ), mouse resistin (mResistin), mouse RELMβ (mRELMβ), mouse RELMγ (mRELMγ), m36B4 and h36B4 are shown in Table 2. The primers for hRELMβ and h36B4 were used as described previously [14,18].

2.6. *Histological analysis*

Colonic tissues were routinely embedded in paraffin; approximately 5 μm-thick slices were obtained from these samples. Slices were stained with hematoxylin and eosin (HE) to compare the number of goblet cells. Immunostaining was performed according to the microwave antigen-retrieval technique, using purified anti-mRELMβ antibody (1:500) and a VECSTATIN ABC kit (Vector labs), following the manufacturer's instructions.

2.7. *Western blotting*

Twenty micrograms of protein extracted from homogenized colonic tissue or 4 μl of serum was boiled in Laemmli sample buffer containing 100 mmol/l dithiothreitol. Samples were subjected to SDS-PAGE, transferred to Hybond-P membranes (GE Healthcare, Bioscience Inc.), and immunoblotted using purified anti-mRELMβ antibody (1:1000). Proteins were visualized with enhanced chemiluminescence (ECL) and exposed to ECL film (GE Healthcare, Bioscience Inc.). The band intensity was analyzed as described previously [16].

2.8. *Statistical analysis*

Stat View-J 5.0 software for windows (SAS Institute Inc.) was used for statistical analysis. Results are expressed as mean ± S.E. In the multiple comparisons, ANOVA followed by the post hoc Fisher's PLSD test was used to compare means between pairs of groups. The unpaired t-test was also used to compare means between pairs of groups.

3. Results

3.1. *Characterizations of feeding groups, energy intake and changes in serum lipid, glucose and insulin levels*

The body weights, epididymal fat weights, glucose levels, insulin levels and serum lipid levels at the start and after 2

Table 2 – Primers used for real-time PCR

	Sense	Antisense
m-Resistin	TCATTTCCCCTCCTTTTCCT	AAGCGACCTGCAGCTTACA
m-RELMα	TCCAGCTAACTATCCCTCCACTGT	CAGTAGCAGTCATCCCAGCA
m-RELMβ	CAAAAAGCTAGAACTGAGCTCCAG	TAGTAATATGAAGACAATGAGTCAGG
m-RELMγ	CTTGCCAATCGAGATGACTG	TTTCCAAGTTGGGATTGTGC
m-36B4	GCTCCAAGCAGATGCAGCA	CCGGATGTGAGGCAGCAG
h RELMβ	CACCCAGGAGCTCAGAGATCTAA	ACGGCCCCATCCTGTACA
h-36B4	CCACGCTGCTGAACATGCT	TCGAACACCTGCTGGATGAC

Table 3a – Characteristics of the dietary groups of the study

	Control	High carbohydrate	High protein	High fat
Body weight (g)	19.2 ± 0.32	19.2 ± 0.15	19.4 ± 0.33	19.2 ± 0.22
Blood glucose (mg/dl)	66.4 ± 3.24	67.8 ± 6.34	64.7 ± 4.21	57.9 ± 3.03
Insulin (ng/ml)	2.91 ± 0.09	3.20 ± 0.31	2.80 ± 0.50	3.72 ± 0.17
Triglyceride (mg/dl)	73.8 ± 5.32	69.6 ± 4.47	76.3 ± 6.56	65.9 ± 3.40
Cholesterol (mg/dl)	82.6 ± 3.07	61.8 ± 6.51	84.6 ± 4.79	80.5 ± 7.27
NEFA (μEq/l)	1.33 ± 0.06	1.28 ± 0.18	1.14 ± 0.07	1.00 ± 0.05

Values are indicated as mean ± S.E. ($n = 4$–6).
No statistically significant differences between the feeding groups were observed.

Table 3b – Characteristics of the dietary groups at the end of the 2-week feeding period

	Control	High carbohydrate	High protein	High fat
Body weight (g)	21.1 ± 0.6	20.4 ± 0.6	19.7 ± 1.0	23.0 ± 0.3
Blood glucose (mg/dl)	84.6 ± 6.0	90.0 ± 8.4	120.6 ± 21.7	125.4 ± 17.0
Insulin (ng/ml)	5.82 ± 1.16	4.47 ± 0.66	4.64 ± 2.70	14.50 ± 3.43*
Triglyceride (mg/dl)	60.7 ± 4.8	49.5 ± 4.6	45.2 ± 9.8	61.2 ± 4.1
Cholesterol (mg/dl)	87.4 ± 6.0	108.1 ± 5.0*	46.2 ± 6.4*	98.3 ± 5.3
NEFA (μEq/l)	0.92 ± 0.09	0.86 ± 0.01	0.94 ± 0.10	0.92 ± 0.04
Epididymal fat (mg)	115.8 ± 16.1	49.6 ± 2.6*	129.1 ± 29.9	404.6 ± 17.0*

$n = 4$–6.
* $p < 0.05$.

weeks of feeding are shown in Tables 3a and 3b, respectively. Body weights, glucose levels and lipid profiles at the beginning of the feeding period did not differ significantly among the groups (Table 3a). Body weights of the three different dietary groups did not differ significantly from that of the control group at the end of the 2-week feeding period, though the high-fat group tended to be heavier (Table 3b). Furthermore, the epididymal fat mass of the high-fat group was significantly larger than that of the control group at the end of the 2-week feeding period (C 115.8 ± 16.1 mg, HF 404.6 ± 17.0 mg; $p < 0.01$) (Table 3b). The high-carbohydrate group had a significantly reduced adipose tissue mass as compared to the control group (C 115.8 ± 16.1 mg, CA 49.6 ± 2.6 mg; $p < 0.05$) (Table 3b).

In contrast to the adipose depot mass, serum total cholesterol was slightly elevated in the high-carbohydrate group by the second week (C 87.4 ± 6.0 mg/dl, CA 108.1 ± 5.0 mg/dl; $p = 0.02$). The high-protein group, however, had significantly lower levels at the end of the second week (C 87.4 ± 6.0 mg/dl, P 46.2 ± 6.4 mg/dl; $p < 0.01$) (Table 3b). Serum non-esterified fatty acids (NEFA) and triglyceride levels did not differ significantly among the groups.

3.2. *Impaired glucose tolerance in the high-fat diet group*

To assess whether these diets impair glucose tolerance, intraperitoneal glucose tolerance tests were performed at the end of the 2-week feeding period, as described in Section 2 (Fig. 1). The high-fat group showed a significantly greater glucose rise than the control group, and showed this serum glucose elevation was sustained beyond the 120 min of the test. No such obvious glucose intolerance was detected in either the high-carbohydrate or the high-protein group.

3.3. *Expression levels of RELMβ and RELMγ in the colon, and of resistin and RELMα in white adipose tissue*

RELMβ expression profiles in fasted and fed states, and the correlations between levels in the colon and ileum are presented in Fig. 2. In the fasted state, the RELMβ protein level was downregulated 43.3 ± 17.2% as compared with that in the fed state (*ad libitum*), which suggests that the diet itself affects RELMβ expression (Fig. 2A and B). There was a positive correlation between RELMβ mRNA levels in the ileum and the colon ($r^2 = 0.604$, $p = 0.0002$), although the RELMβ mRNA level

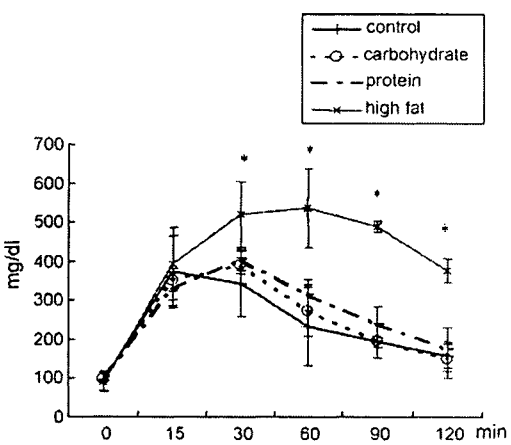

Fig. 1 – Impaired glucose tolerance in the high-fat diet group. The results of intra-peritoneal glucose tolerance tests done at the end of the second week are shown. Asterisks (*) denote glucose values significantly different from those of the control group. Bars indicate standard errors ($n = 3$–4).

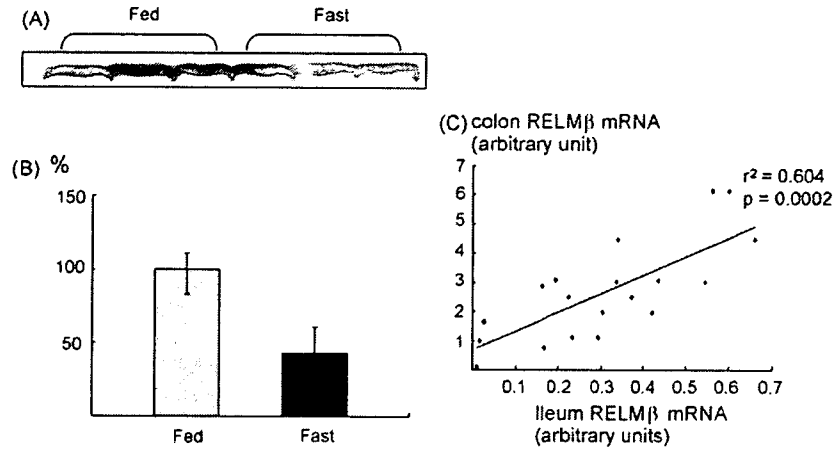

Fig. 2 – Altered expressions of RELMβ in fed and fasted states and comparison of RELMβ expressions in the ileum and colon. The protein level is shown as band (A), quantification as band (B), using NIH image. Asterisks (*) denote values in the state, which are significantly different from those in the fed state. Bars indicate standard errors (n = 3). The RELMβ mRNA level is shown in a scatter plot. The X-axis represents RELMβ from the ileum, the Y-axis that from the colon. Scales of the two are arbitrary but the values correspond to each other.

in the colon was more variable than that in the ileum, being up to 10 times higher (Fig. 2C). A positive correlation between RELMβ levels in serum and the colon was demonstrated previously [16].

As shown in Fig. 3A, interestingly, it was revealed that the high-carbohydrate and high-protein diets had markedly decreased RELMβ mRNA expression by the end of the 2-week feeding period (C 1.0 ± 0.34, CA 0.002 ± 0.001; $p = 0.02$, P 0.09 ± 0.06; $p < 0.01$) in the colon, while RELMβ mRNA expression in the high-fat group was slightly higher than that of the control group, but this difference was not statistically significant (Fig. 3A). In the ileum and serum, the same tendency was observed, as shown in Fig. 3B and C, although only serum RELMβ in the high protein group changed significantly (C 1.00 ± 0.15, CA 0.67 ± 0.33, P 0.46 ± 0.02, $p < 0.02$, F 1.31 ± 0.16 in serum, C 1.00 ± 0.24, CA 0.73 ± 0.10, P 0.68 ± 0.06, F 0.95 ± 0.23 in the ileum). These results suggest a strong influence of nutritional components on RELMβ expression in the colon. Furthermore, a single feeding produced no significant change in RELMβ mRNA (1.00 ± 0.13, CA 1.06 ± 0.23, P 0.84 ± 0.04 or F 0.82 ± 0.07) in the colon. The RELMβ mRNA level was changed by the diet itself, although repetitive and chronic stimulation was needed for those dietary components to change the RELMβ mRNA level.

The resistin mRNA analysis of white adipose tissue conducted during the second week of the feeding period, showed no significant differences among the groups (Fig. 4A). The RELMα mRNA expression levels in white adipose tissue

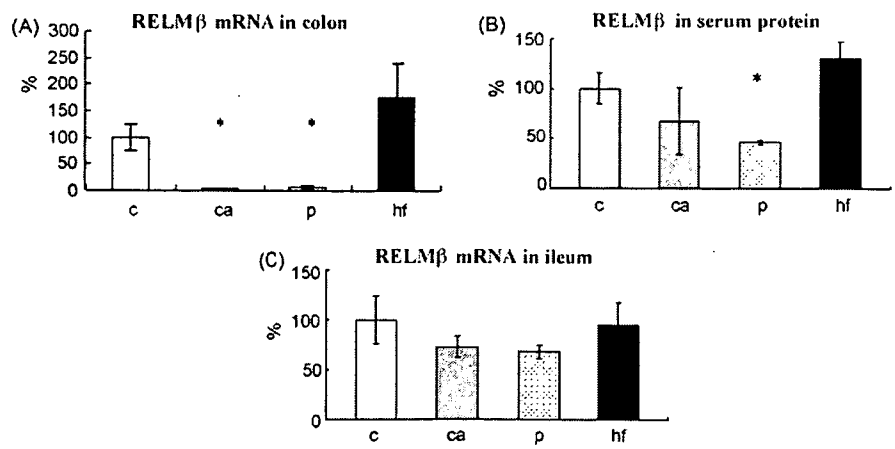

Fig. 3 – Altered expressions of RELMβ in the colon, ileum and serum in response to various dietary compositions. The mice were given a control, high-carbohydrate, high-protein or high-fat diet for 2 weeks. RELMβ expressions in the colon (A), serum (B) and ileum (C) were investigated and the data are presented as percentages of the control group values. Asterisks (*) denote values significantly different from those of the control group. Bars indicate standard errors (n = 4–6).

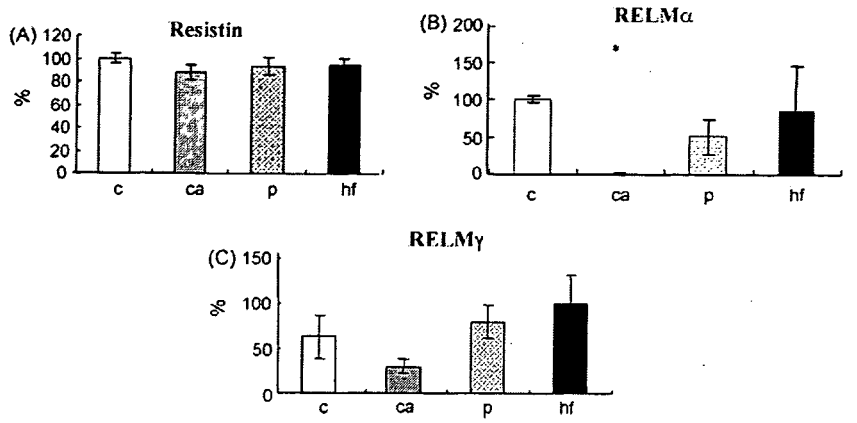

Fig. 4 – Expressions of resistin and RELMα mRNAs in adipose tissue and RELMγ in the colon in response to various dietary compositions. The mice were given a control, high-carbohydrate, high-protein or high-fat diet for 2 weeks. The expressions of resistin (A) and RELMα (B) mRNAs in adipose tissue and RELMγ (C) in the colon were investigated and the data are presented as percentages of the control group values. Asterisks (*) denote values significantly different from those of the control group. Bars indicate standard errors (n = 4–6).

are presented in Fig. 4B. RELMγ mRNA expressions in the colon did not differ among the dietary groups (Fig. 4C). Two-week feeding of a high-carbohydrate diet significantly suppressed RELMα expression as compared to the control group, while the high-protein and high-fat diets had no marked effects.

3.4. *Histological analysis*

Representative RELMβ immunohistochemistry of the colon, the major RELMβ production site, for each dietary group, is presented in Fig. 5. The high-carbohydrate and high-protein

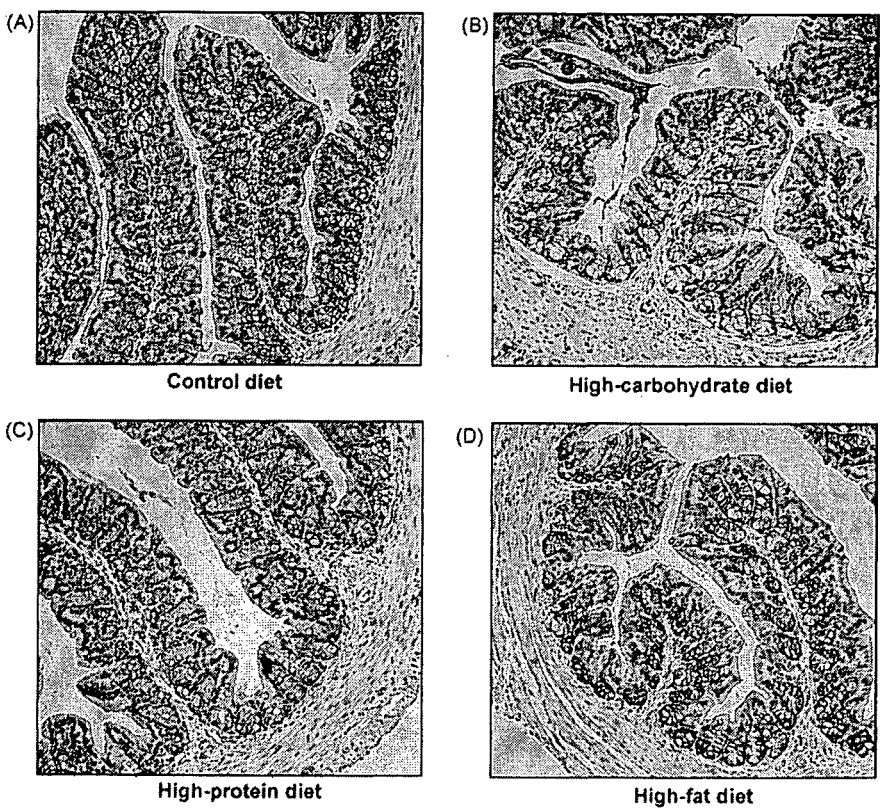

Fig. 5 – Colonic Immunohistochemistry of RELMβ. Colonic immunohistochemistry of RELMβ (magnification 100×) for each dietary group is shown. RELMβ is identifiable by its brown appearance. (A) Control diet, (B) high-carbohydrate diet, (C) high-protein diet, (D) high-fat diet.

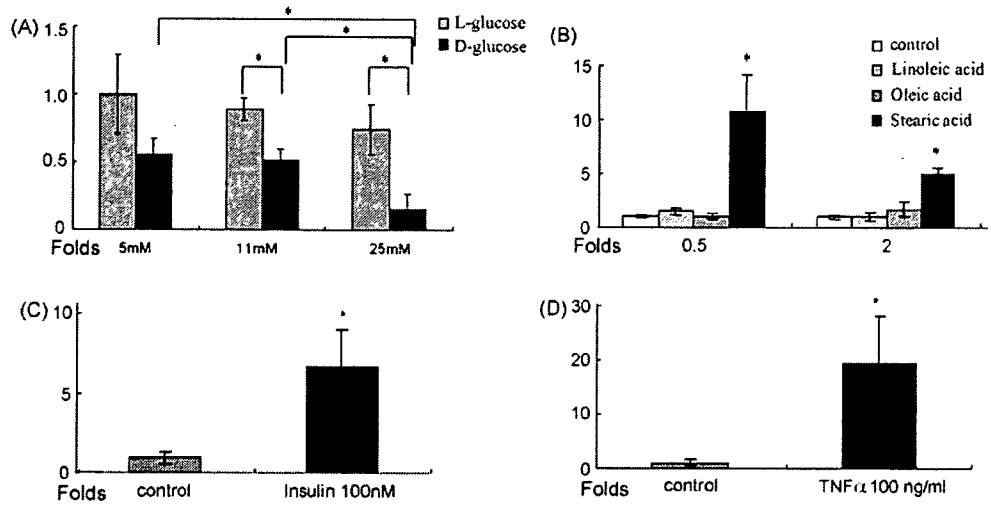

Fig. 6 – hRELMβ mRNA expression in LS174T cells with different stimuli. The hRELMβ mRNA expressions in LS174T cells after 24 h stimulation, with the agents shown at the indicated concentrations, are presented. (A) The cells were incubated with D-glucose or L-glucose at concentrations of 5 mM, 11 mM and 25 mM. The data are presented as the fold increase compared to the L-glucose group. (B) The cells were incubated with or without linoleic acid, oleic acid or stearic acid at concentrations of 0.5 and 2 mM. The data are shown as fold increases compared to the group without stimulation. (C) The cells were incubated with or without 100 nM insulin. (D) The cells were incubated with or without 100 ng/ml TNFα. Data from four separate experiments are presented and the bars indicate standard errors. The asterisks (*) denote values significantly different from those of the control group.

diet groups showed significantly less RELMβ expression than the control and high-fat diet groups. HE-stained preparations from all dietary groups were compared for the number of goblet cells. The absence of significant differences in numbers of intestinal goblet cells, among the groups, was also confirmed.

3.5. *Changes in hRELMβ mRNA expression in a human colon cancer cell line with various stimulations*

Expressions of hRELMβ mRNA in the human colon cancer cell line LS174T, were compared after stimulation with D-glucose or L-glucose, insulin, TNFα and three types of FFA, as described in Section 2. The results are presented in Fig. 6. Stimulation with D-glucose at 5, 11 and 25 mM significantly reduced the RELMβ mRNA expression in a concentration dependent manner (Fig. 6A). The three FFA exerted different effects on mRNA expression. Stearic acid stimulation resulted in marked upregulation of the RELMβ mRNA level (0.5 mM stearic acid, 10.7 ± 3.3 fold; $p < 0.01$, 2.0 mM stearic acid, 3.4 ± 0.38 fold; $p < 0.01$), while linoleic and oleic acids had no significant effects (Fig. 6B).

Stimulation with 100 nM insulin induced a 6.7-fold increase in mRNA expression ($p < 0.01$) (Fig. 6C). TNFα stimulation markedly increased RELMβ mRNA expression, by approximately 20 fold ($p < 0.01$) (Fig. 6D).

4. Discussion

One major factor contributing to Type 2 diabetes mellitus is insulin resistance, and obesity is known to be the most common factor inducing insulin resistance. Pathophysiological states (*i.e.* insulin resistance, obesity, and low-grade inflammation) are major and synergistic components of the metabolic syndrome. It was recently demonstrated that adipocytes are not only a lipid depot site, but also actively produce and secrete hormones and cytokines [19]. Resistin is one of these adipocyte-derived proteins and was suggested to play a role in the development of insulin resistance [4].

In addition, it was revealed that resistin and three structurally related RELMs constitute a resistin family [2,3,14]. Only RELMβ among these three RELMs is present in humans. Intestinal RELMβ secretion is reportedly increased in response to bacterial colonization [14] and has been suggested to be involved in the defense mechanism against nematode infestation in mice [15]. On the other hand, administration of RELMβ via the bloodstream induces acute hepatic insulin resistance [20], and transgenic mice over-expressing RELMβ in the liver were shown to exhibit hyperglycemia, hyperlipidemia and fatty liver [17]. These findings suggest that RELMβ is involved in both inflammatory responses intrinsic to the intestine and insulin resistance, particularly in the liver, and therefore may be an important link between these two pathophysiological states. Taking the aforementioned background factors into consideration, we carried out this study to investigate the regulatory effects of various nutritional factors in food on the expressions of RELMβ and other isoforms.

The effects of different nutritional components of diets are now receiving attention, especially in relation to obesity. With the intention of preventing and treating obesity and related diseases, intervention trials have been undertaken [21,22]. Diets rich in carbohydrate and low in fat have been employed, and have been found to reduce the incidence of diabetes by up

to 60%. Diets of similar composition are also recommended by medical societies for the treatment of diabetes [23,24]. Another study revealed that a high-protein diet resulted in substantial and sustained improvements in waist circumference, triglycerides and insulin, whereas with a high carbohydrate diet these changes were more modest [25]. In patients with Type 2 diabetes, a high protein diet reportedly improved glucose metabolism, due to the stimulatory effect of protein on insulin secretion [26].

In the present study, neither the high-carbohydrate nor the high-protein diet for 2 weeks induced either hyperinsulinemia or hyperglycemia in the fasting condition, nor was there any obvious glucose tolerance impairment in mice. Furthermore, epididymal fat tissue masses in both groups were reduced or were similar to those of the control group. These results are in a good accordance with the reported observations in a clinical trial [25]. In this study, we first demonstrated RELMβ expression in mice to be strongly influenced by whether the animals were fasted or fed, and differences in dietary nutritional composition, while resistin expression in adipose tissues did not differ significantly among the dietary groups. Resistin levels in white adipose tissue are reportedly higher in insulin resistant rodent models [4], though others have described contrasting observations [6–8]. Post-transcriptional and/or post-translational modifications, that consequently affect the secretion rate of the protein, have been suggested as possible explanations for this discrepancy.

Since RELMβ is the only RELM in humans, we focused on the regulation of colonic RELMβ expression, which was significantly suppressed in both the high-protein and the high-carbohydrate group. The histological investigations ruled out suppressed RELMβ expression due to a reduced number of goblet cells, and indicated that RELMβ secretion is markedly influenced by nutrients. Therefore, we speculate that protein and carbohydrate exert suppressive effects, or alternatively that an as yet unknown lipid, induces RELMβ expression. We also considered the possible involvement of insulin and TNFα, serum concentrations of which are increased in high-fat diet-induced insulin resistance. To examine these possibilities, a human colon cancer cell line, LS174T, which has been shown to express human RELMβ (RELMβ) under basal conditions [14], was subjected to various culture conditions. The initial incubation of these cells with D-glucose induced significantly lower RELMβ expression, in a D-glucose concentration dependent manner, than the same L-glucose concentrations. Subsequently, it was revealed that only the saturated FFA, *i.e.* stearic acid, had significant inducing effects on RELMβ mRNA expression, while the other two free fatty acids had little impact.

We also demonstrated insulin and TNFα to markedly increase RELMβ expression. Induction of RELMβ expression by TNFα is an observation in good accordance with previous study results showing induction of RELMβ expression by Th2 cytokines such as Il-4 and IL-13 [15]. Furthermore, the presence of several STAT6 and NFκB elements in the promoter region of human RELMβ was disclosed by sequence analysis [14].

Taking these results together, we can suggest possible mechanisms underlying diet-induced RELMβ regulation. First, repetitive and chronic stimulation by certain free fatty acids, such as stearic acid, or glucose, *per se*, increased and decreased RELMβ expression, respectively. Second, although no supporting data were obtained in this study, it is reasonable to speculate that the different nutritional compositions of foods would affect bacterial colonization in the colon, and that differences in bacterial colonization might affect RELMβ expression either directly or indirectly (*i.e.* systemic hormonal changes) through local Th2 cytokine production. Finally, a high-fat diet enlarges adipocytes, which in turn induces the secretion of various proteins such as TNFα while high-carbohydrate and high-protein diets reduce adipocyte size. In addition, FFA also reportedly induces the release of TNFα from macrophages [27]. TNFα secreted by adipocytes and macrophages would then induce the expression of RELMβ. We speculate that some or all of these mechanisms are involved in the nutrient-induced regulation of RELMβ. The high concentrations of RELMβ secreted by the intestines would reach the liver via the blood stream and thus contribute to the development of insulin resistance.

In conclusion, this study has clearly shown intestinal RELMβ expression to be strongly influenced by the nutritional compositions of foods. Up-regulation by inflammatory mediators, together with the previous demonstration of the RELMβ association with insulin resistance, suggests a role for this protein as a cytokine contributing to the pathogenesis of insulin resistance and thereby to that of the metabolic syndrome.

REFERENCES

[1] C.M. Steppan, E.J. Brown, C.M. Wright, S. Bhat, R.R. Banerjee, C.Y. Dai, et al., A family of tissue-specific resistin-like molecules, Proc. Natl. Acad. Sci. U.S.A. 98 (2001) 502–506.

[2] B. Gerstmayer, D. Kusters, S. Gebel, T. Muller, E. Van Miert, K. Hofmann, et al., Identification of RELMgamma, a novel resistin-like molecule with a distinct expression pattern, Genomics 81 (2003) 588–595.

[3] I.N. Holcomb, R.C. Kabakoff, B. Chan, T.W. Baker, A. Gurney, W. Henzel, et al., FIZZ1, a novel cysteine-rich secreted protein associated with pulmonary inflammation, defines a new gene family, EMBO J. 19 (2000) 4046–4055.

[4] C.M. Steppan, S.T. Bailey, S. Bhat, E.J. Brown, R.R. Banerjee, C.M. Wright, et al., The hormone resistin links obesity to diabetes, Nature 409 (2001) 307–312.

[5] R.R. Banerjee, S.M. Rangwala, J.S. Shapiro, A.S. Rich, B. Rhoades, Y. Qi, et al., Regulation of fasted blood glucose by resistin, Science 303 (2004) 1195–1198.

[6] J.M. Way, C.Z. Gorgun, Q. Tong, K.T. Uysal, K.K. Brown, W.W. Harrington, et al., Adipose tissue resistin expression is severely suppressed in obesity and stimulated by peroxisome proliferator-activated receptor gamma agonists, J. Biol. Chem. 276 (2001) 25651–25653.

[7] G. Milan, M. Granzotto, A. Scarda, A. Calcagno, C. Pagano, G. Federspil, et al., Resistin and adiponectin expression in visceral fat of obese rats: effect of weight loss, Obes. Res. 10 (2002) 1095–1103.

[8] C.C. Juan, L.C. Au, V.S. Fang, S.F. Kang, Y.H. Ko, S.F. Kuo, et al., Suppressed gene expression of adipocyte resistin in an insulin-resistant rat model probably by elevated free fatty acids, Biochem. Biophys. Res. Commun. 289 (2001) 1328–1333.

[9] I. Nagaev, U. Smith, Insulin resistance and type 2 diabetes are not related to resistin expression in human fat cells or

skeletal muscle, Biochem. Biophys. Res. Commun. 285 (2001) 561–564.
[10] K.H. Kim, K. Lee, Y.S. Moon, H.S. Sul, A cysteine-rich adipose tissue-specific secretory factor inhibits adipocyte differentiation, J. Biol. Chem. 276 (2001) 11252–11256.
[11] T. Liu, H. Jin, M. Ullenbruch, B. Hu, N. Hashimoto, B. Moore, et al., Regulation of found in inflammatory zone 1 expression in bleomycin-induced lung fibrosis: role of IL-4/IL-13 and mediation via STAT-6, J. Immunol. 173 (2004) 3425–3431.
[12] A.M. Chumakov, T. Kubota, S. Walter, H.P. Koeffler, Identification of murine and human XCP1 genes as C/EBP-epsilon-dependent members of FIZZ/resistin gene family, Oncogene 23 (2004) 3414–3425.
[13] T. Schinke, M. Haberland, A. Jamshidi, P. Nollau, J.M. Rueger, M Amling, Cloning and functional characterization of resistin-like molecule gamma, Biochem. Biophys. Res. Commun. 314 (2004) 356–362.
[14] W. He, M.L. Wang, H.Q. Jiang, C.M. Steppan, M.E. Shin, M.C. Thurnheer, et al., Bacterial colonization leads to the colonic secretion of RELMbeta/FIZZ2, a novel goblet cell-specific protein, Gastroenterology 125 (2003) 1388–1397.
[15] D.W.M. Artis, S.A. Keilbaugh, W. He, M. Brenes, G.P. Swain, P.A. Knight, D.D. Donaldson, et al., RELMbeta/FIZZ2 is a goblet cell-specific immune-effector molecule in the gastrointestinal tract, Proc. Natl. Acad. Sci. U.S.A. 101 (2004) 13596–13600.
[16] N. Shojima, T. Ogihara, K. Inukai, M. Fujishiro, H. Sakoda, A. Kushiyama, et al., Serum concentrations of resistin-like molecules beta and gamma are elevated in high-fat-fed and obese db/db mice, with increased production in the intestinal tract and bone marrow, Diabetologia 48 (2005) 984–992.
[17] A. Kushiyama, N. Shojima, T. Ogihara, K. Inukai, H. Sakoda, M. Fujishiro, et al., Resistin like molecule beta activates MAPKs, suppresses insulin signaling in hepatocytes and induces diabetes, hyperlipidemia and fatty liver in transgenic mice on a high-fat diet, J. Biol. Chem. 280 (2005) 42016–42025.
[18] S.R. Krutzik, M.T. Ochoa, P.A. Sieling, S. Uematsu, Y.W. Ng, A. Legaspi, et al., Activation and regulation of Toll-like receptors 2 and 1 in human leprosy, Nat. Med. 9 (2003) 525–532.
[19] B.B. Kahn, J.S. Flier, Obesity and insulin resistance, J. Clin. Invest. 106 (2000) 473–481.
[20] M.W. Rajala, S. Obici, P.E. Scherer, L. Rossetti, Adipose-derived resistin and gut-derived resistin-like molecule-beta selectively impair insulin action on glucose production, J. Clin. Invest. 111 (2003) 225–230.
[21] J. Tuomilehto, J. Lindstrom, J.G. Eriksson, T.T. Valle, H. Hamalainen, P. Ilanne-Parikka, et al., Prevention of type 2 diabetes mellitus by changes in lifestyle among subjects with impaired glucose tolerance, N. Engl. J. Med. 344 (2001) 1343–1350.
[22] W.C. Knowler, E. Barrett-Connor, S.E. Fowler, R.F. Hamman, J.M. Lachin, E.A. Walker, et al., Reduction in the incidence of type 2 diabetes with lifestyle intervention or metformin, N. Engl. J. Med. 346 (2002) 393–403.
[23] M.J. Franz, J.P. Bantle, C.A. Beebe, J.D. Brunzell, J.L. Chiasson, A. Garg, et al., Evidence-based nutrition principles and recommendations for the treatment and prevention of diabetes and related complications, Diabetes Care 26 (Suppl. 1) (2003) S51–S61.
[24] The Diabetes and Nutrition Study Group (DNSG) of the European Association for the Study of Diabetes (EASD), 1999, Recommendations for the nutritional management of patients with diabetes mellitus, Eur. J. Clin. Nutr. 54 (2000) 353–355.
[25] K.A. McAuley, K.J. Smith, R.W. Taylor, R.T. McLay, S.M. Williams, J.I. Mann, Long-term effects of popular dietary approaches on weight loss and features of insulin resistance, Int. J. Obes. (Lond) (2005) 342–349.
[26] F.Q. Nuttall, M.C. Gannon, Metabolic response of people with type 2 diabetes to a high protein diet, Nutr. Metab. (Lond) 1 (2004) 6.
[27] T.N.J. Suganami, Y. Ogawa, A paracrine loop between adipocytes and macrophages aggravates inflammatory changes: role of free fatty acids and tumor necrosis factor-alpha, Arterioscler. Thromb. Vasc. Biol. 25 (2005) 2062–2068.

Cell Metabolism

ATF4-Mediated Induction of 4E-BP1 Contributes to Pancreatic β Cell Survival under Endoplasmic Reticulum Stress

Suguru Yamaguchi,[1,3] Hisamitsu Ishihara,[1,*] Takahiro Yamada,[1] Akira Tamura,[1] Masahiro Usui,[1] Ryu Tominaga,[1] Yuichiro Munakata,[1] Chihiro Satake,[1] Hideki Katagiri,[2] Fumi Tashiro,[4] Hiroyuki Aburatani,[5] Kyoko Tsukiyama-Kohara,[6] Jun-ichi Miyazaki,[4] Nahum Sonenberg,[7] and Yoshitomo Oka[1]

[1]Division of Molecular Metabolism and Diabetes

[2]Division of Advanced Therapeutics for Metabolic Diseases, Center for Translational and Advanced Animal Research Tohoku University Graduate School of Medicine, Sendai, Miyagi 980-8575, Japan

[3]Institute for International Advanced Research and Education, Tohoku University, Sendai, Miyagi 980-8578, Japan

[4]Division of Stem Cell Regulation Research, Osaka University Graduate School of Medicine, Suita, Osaka 565-0871, Japan

[5]Research Center for Advanced Science and Technology, University of Tokyo, Tokyo 153-8904, Japan

[6]Department of Experimental Phylaxiology, Faculty of Medical and Pharmaceutical Sciences, Kumamoto University, Kumamoto 860-8556, Japan

[7]Department of Biochemistry and McGill Cancer Centre, McGill University, Montreal, QC H3G 1Y6, Canada

*Correspondence: hisamitsu-ishihara@mail.tains.tohoku.ac.jp

DOI 10.1016/j.cmet.2008.01.008

SUMMARY

Endoplasmic reticulum (ER) stress-mediated apoptosis may play a crucial role in loss of pancreatic β cell mass, contributing to the development of diabetes. Here we show that induction of 4E-BP1, the suppressor of the mRNA 5′ cap-binding protein eukaryotic initiation factor 4E (eIF4E), is involved in β cell survival under ER stress. 4E-BP1 expression was increased in islets under ER stress in several mouse models of diabetes. The *Eif4ebp1* gene encoding 4E-BP1 was revealed to be a direct target of the transcription factor ATF4. Deletion of the *Eif4ebp1* gene increased susceptibility to ER stress-mediated apoptosis in MIN6 β cells and mouse islets, which was accompanied by deregulated translational control. Furthermore, *Eif4ebp1* deletion accelerated β cell loss and exacerbated hyperglycemia in mouse models of diabetes. Thus, 4E-BP1 induction contributes to the maintenance of β cell homeostasis during ER stress and is a potential therapeutic target for diabetes.

INTRODUCTION

Recent studies have shown decreased pancreatic β cell mass to be a common feature of subjects with type 2 diabetes mellitus (Butler et al., 2003). Susceptibility to stress-induced apoptosis may underlie β cell loss. Translational regulation is an essential strategy by which cells cope with stress conditions (Clemens, 2001). Translation of eukaryotic mRNA is regulated primarily at the level of initiation. Translational initiation begins with formation of a ternary complex composed of the methionine-charged initiator tRNA, eukaryotic initiation factor 2 (eIF2), and GTP (Holcik and Sonenberg, 2005). The ternary complex then binds to the 40S ribosomal subunit and several other initiation factors, generating the 43S preinitiation complex. The mRNA 5′ cap-binding protein eIF4E associates with eIF4A and eIF4G to form the eIF4F complex and interacts with the 5′ cap structure of the mRNA. The eIF4F complex then recruits the 43S preinitiation complex to the mRNA, allowing the complex to scan toward the initiator AUG codon. The two best characterized regulatory steps in this translational control are formation of the ternary complex and assembly of the eIF4F complex. Phosphorylation of the α subunit of eIF2 (eIF2α) prevents ternary complex formation and thereby suppresses global translation. In addition, eIF4E-binding proteins (4E-BPs) inhibit eIF4F assembly by competitively displacing eIF4G from eIF4E. Global translational suppression through eIF2α phosphorylation is a mechanism shared among different stress-response pathways. Depending on the nature of the stress stimulus, eIF2α can be phosphorylated by four different kinases (Holcik and Sonenberg, 2005). Global attenuation of protein biosynthesis then paradoxically increases expression of several proteins, including the transcription factor ATF4 (Harding et al., 2000).

Because of their high insulin secretory activity, β cells are vulnerable to endoplasmic reticulum (ER) stress, a condition of disrupted ER homeostasis due to accumulation of misfolded proteins (Schroder and Kaufman, 2005). Cells respond to ER stress by activating an adaptive cellular response known as the unfolded protein response (UPR). Under ER stress conditions, global translation is suppressed through eIF2α phosphorylation by an ER-resident kinase, PERK. The importance of PERK-mediated translational suppression has been demonstrated in infancy-onset diabetes and skeletal defects caused by loss of PERK in humans (Delepine et al., 2000) and mice (Harding et al., 2001; Zhang et al., 2002). However, the roles of translational control through inhibition of eIF4F assembly by 4E-BPs under stress conditions, including ER stress, have yet to be fully clarified. Herein, we have studied roles of 4E-BP1,

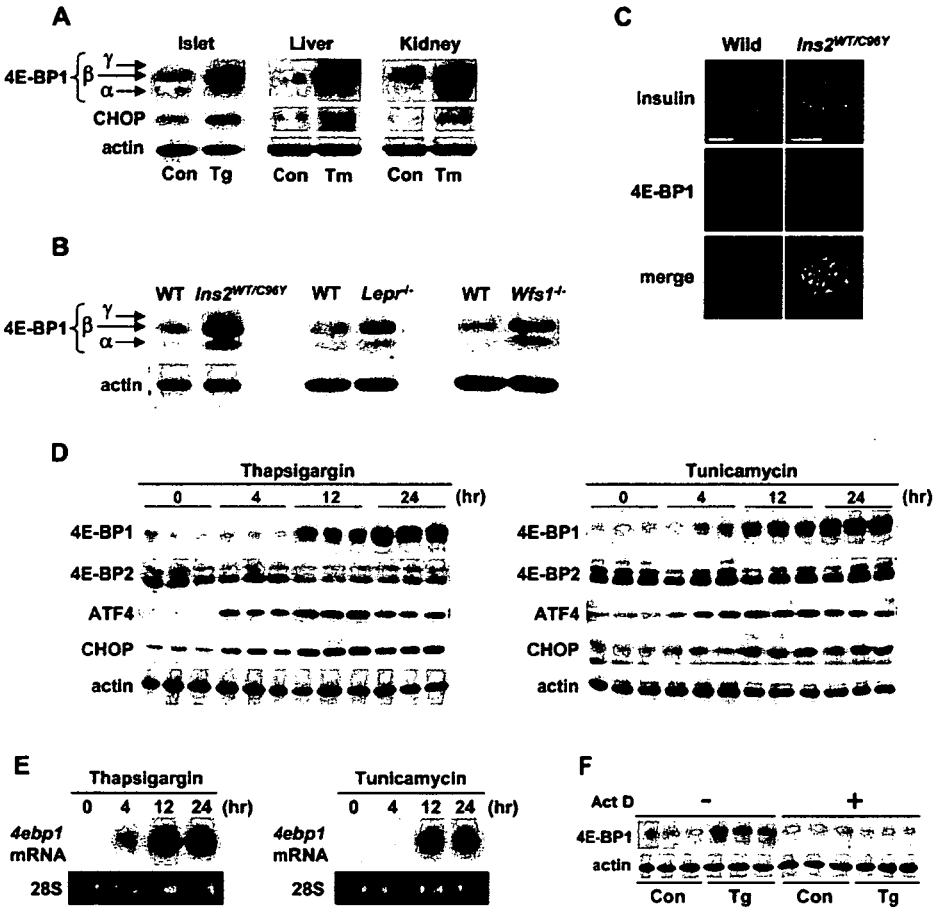

Figure 1. ER Stress Induces 4E-BP1 Expression

(A) Expression of 4E-BP1 protein in isolated islets treated with vehicle (0.05% DMSO) control (Con) or 0.5 μM thapsigargin (Tg) for 12 hr. 4E-BP1 expression was also examined in the livers and kidneys of mice that had received intraperitoneal injections of tunicamycin (Tm) 96 hr previously.

(B) Expression of 4E-BP1 protein in islets from wild-type (WT), *Ins2*$^{WT/C96Y}$, *Lepr* $^{-/-}$, and *Wfs1* $^{-/-}$ mice.

(C) Immunostaining of pancreatic sections from WT and *Ins2*$^{WT/C96Y}$ mice using anti-insulin and anti-4E-BP1 antibodies. Scale bars = 50 μm.

(D and E) Time courses of 4E-BP1, 4E-BP2, ATF4, and CHOP expression (D) and *4ebp1* mRNA expression (E) in MIN6 cells treated with thapsigargin (left panel) or tunicamycin (right).

(F) Inhibition of 4E-BP1 induction by actinomycin D (1 μg/ml) in MIN6 cells treated with thapsigargin for 12 hr.

one of three isoforms of the 4E-BP family, in β cells under ER stress.

RESULTS

ER Stress Induces 4E-BP1

4E-BP1 protein is present in three forms with different phosphorylation states. The hypophosphorylated α and β forms are active and the hyperphosphorylated γ form is inactive in terms of eIF4E binding. Expression of 4E-BP1 protein, especially the hypophosphorylated forms, was markedly induced, with an increase in CHOP, a stress marker protein, in isolated islets treated with thapsigargin (an ER Ca^{2+} pump inhibitor causing ER stress) (Figure 1A). 4E-BP1 induction was also observed in liver and kidneys of mice administered tunicamycin (a protein glycosylation inhibitor), another ER stress inducer (Figure 1A).

Furthermore, 4E-BP1 protein expression was markedly increased in *Ins2*$^{WT/C96Y}$ islets (Figures 1B and 1C), in which misfolded insulin molecules with a C96Y mutation cause ER stress (Wang et al., 1999). Islets from leptin receptor null (*Lepr*$^{-/-}$) mice, which have been shown to suffer from ER stress (Laybutt et al., 2007), also exhibited increased 4E-BP1 expression (Figure 1B). The *Wfs1* $^{-/-}$ mouse (Ishihara et al., 2004) is a model of Wolfram syndrome, which is characterized by juvenile-onset diabetes mellitus and optic atrophy and is caused by *WFS1* mutations (Inoue et al., 1998; Strom et al., 1998). WFS1-deficient islets are affected by chronic ER stress (Ishihara et al., 2004; Riggs et al., 2005). Again, 4E-BP1 protein was increased in *Wfs1* $^{-/-}$ islets (Figure 1B).

Induction of 4E-BP1 by ER stress was also observed in insulinoma MIN6 cells (Miyazaki et al., 1990) (Figure 1D). Expression of 4E-BP2, another member of the 4E-BP family, remained unchanged. While expression of ATF4 and CHOP peaked at 12 hr after treatment with thapsigargin or tunicamycin, 4E-BP1 protein was further increased at 24 hr posttreatment (Figure 1D). 4E-BP1 protein induction appeared to result from transcriptional

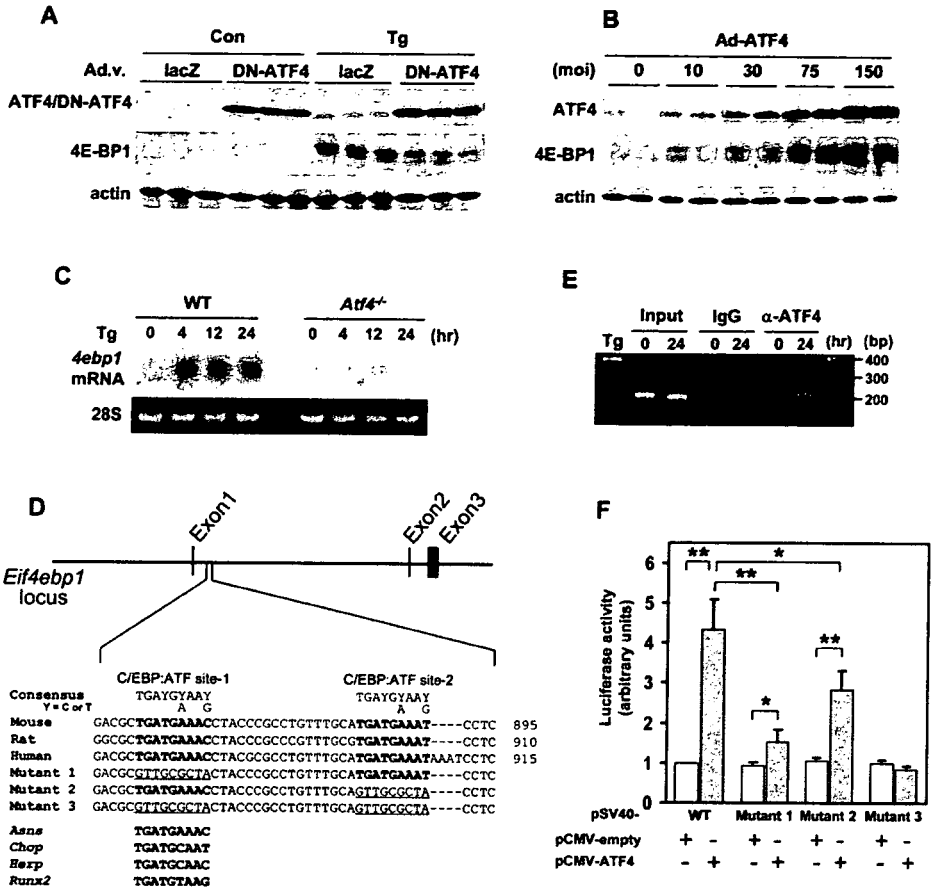

Figure 2. *Eif4ebp1* Is a Direct Target of ATF4

(A) Suppression of thapsigargin (Tg, 0.5 μM)-induced 4E-BP1 expression by dominant-negative ATF4 (DN-ATF4). MIN6 cells were infected with an adenovirus expressing either lacZ or DN-ATF4. Two days later, the cells were treated with vehicle (0.05% DMSO) control (Con) or Tg for 12 hr.

(B) 4E-BP1 expression in MIN6 cells infected with an adenovirus expressing wild-type ATF4 at the indicated multiplicity of infection (moi).

(C) *4ebp1* mRNA levels in wild-type and *Atf4* $^{-/-}$ MEFs treated with thapsigargin.

(D) C/EBP:ATF composite sites in intron 1 of the *Eif4ebp1* gene. Mouse, rat, and human *Eif4ebp1* gene segments are aligned with ATF4 binding sequences in several genes. Numbers are positions relative to A of the initial ATG codon. *Asns*, asparagine synthetase; *Herp*, homocysteine-induced ER protein; *Runx2*, runt-related transcription factor 2.

(E) Chromatin immunoprecipitation assay of MIN6 cells treated with thapsigargin. DNAs precipitated with nonspecific or anti-ATF4 IgG were amplified using primers for the *Eif4ebp1* intron 1 region.

(F) ATF4 induction of luciferase reporters with the *SV40* promoter and an *Eif4ebp1* gene segment with C/EBP:ATF composite sites or their mutants shown in (D). MIN6 cells were transfected with luciferase reporters together with either pCMV-empty or pCMV-ATF4. Error bars represent SEM. n = 4; $^{*}p < 0.05$, $^{**}p < 0.01$.

activation since *4ebp1* mRNA levels were also increased by these ER stress inducers (Figure 1E) and the transcriptional inhibitor actinomycin D completely blocked 4E-BP1 induction by thapsigargin (Figure 1F).

ATF4 Directly Activates the *Eif4ebp1* Gene

MIN6 cells were infected with recombinant adenoviruses expressing dominant-negative (DN) forms of transcription factors involved in the UPR. Expression of DN-ATF4 (He et al., 2001) (Figure 2A), but not DN-ATF6 or DN-XBP1 (see Figure S1 available online), suppressed 4E-BP1 induction by thapsigargin. Conversely, expression of wild-type ATF4 dramatically induced 4E-BP1 expression (Figure 2B). Furthermore, *4ebp1* mRNA levels were not increased by thapsigargin in *Atf4* $^{-/-}$ murine embryonic fibroblasts (MEFs) (Harding et al., 2003) (Figure 2C).

A survey of the mouse *Eif4ebp1* gene using a luciferase assay identified a segment in intron 1 that conferred thapsigargin sensitivity to a luciferase reporter (Figure S2). Indeed, we found two potential ATF4 binding sequences (C/EBP:ATF composite sites) in this segment (Figure 2D). Chromatin immunoprecipitation (ChIP) assays revealed that ATF4 binds this segment (Figure 2E). Furthermore, cotransfection of a luciferase reporter containing the C/EBP:ATF sites with an ATF4-expressing plasmid increased luciferase activity by 4.3-fold (Figure 2F). Disruption of the upstream C/EBP:ATF site (mutant 1) or the downstream site (mutant 2) decreased the ATF4-mediated increase in luciferase activity by 83% or 47%, respectively, and disruption of both (mutant 3) completely abolished the increase (Figure 2F).

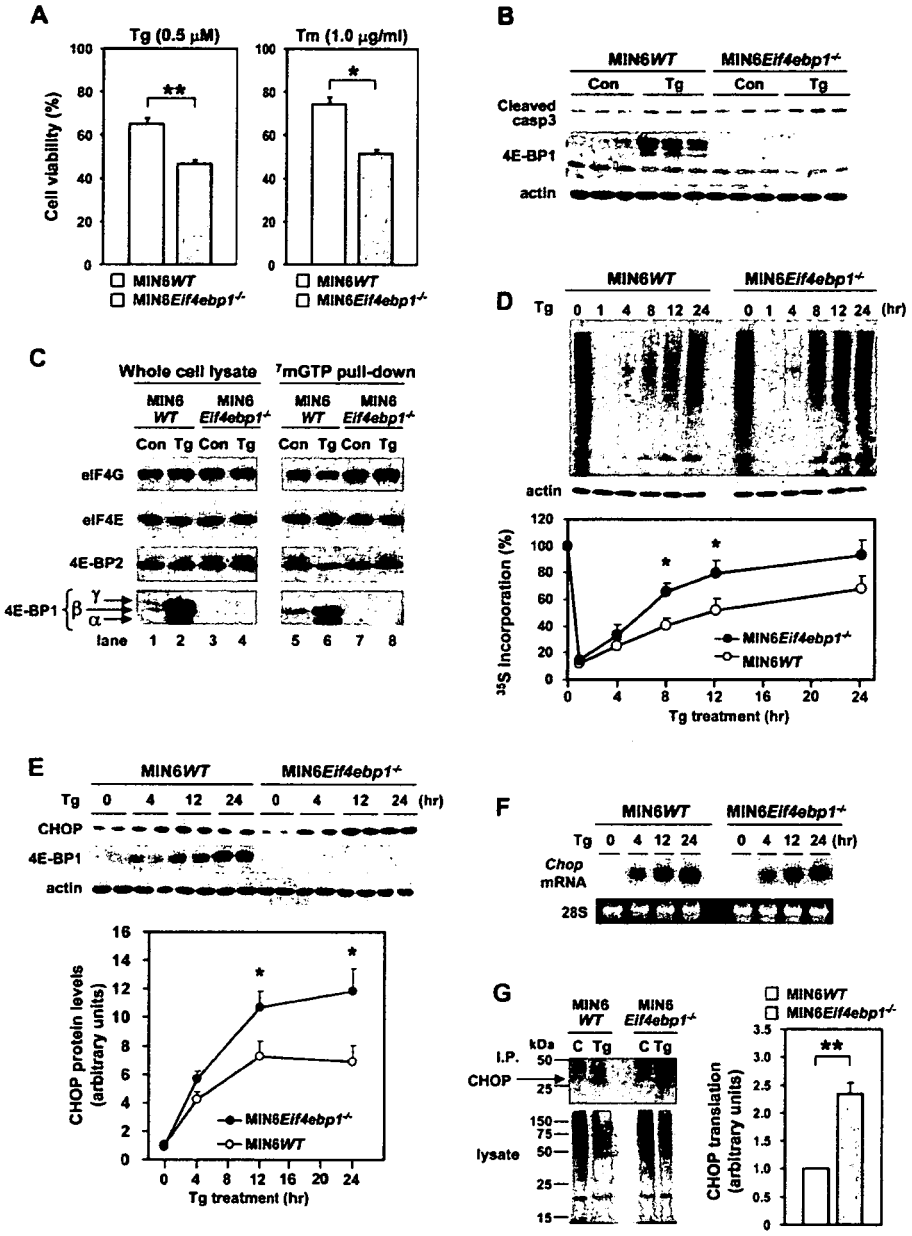

Figure 3. 4E-BP1-Deficient Cells Exhibit Increased Apoptosis Susceptibility with Deregulated Translational Control

(A) Viability of MIN6*WT* and MIN6*Eif4ebp1* $^{-/-}$ cells treated with 0.5 μM thapsigargin (Tg) or 1.0 μg/ml tunicamycin (Tm) for 36 hr, normalized to MIN6*WT* cells treated with vehicle (0.05% DMSO). n = 3–4.

(B) Immunoblot of cleaved caspase-3 in MIN6*WT* and MIN6*Eif4ebp1* $^{-/-}$ cells treated with vehicle control (Con) or thapsigargin for 24 hr.

(C) Immunoblot analysis of 4E-BP1, 4E-BP2, eIF4E, and eIF4G in whole-cell lysates (left) or in a complex associated with ^{7}mGTP-Sepharose (right) in cells treated with thapsigargin for 24 hr.

(D) [^{35}S]methionine/cysteine incorporation during a 15 min pulse labeling in MIN6*WT* and MIN6*Eif4ebp1* $^{-/-}$ cells pretreated with thapsigargin for the indicated periods. Ten percent of the lysates were also probed with an anti-actin antibody. A representative autoradiogram is shown in the upper panel; data from three experiments are summarized in the lower panel.

(E) Increased CHOP induction in MIN6*Eif4ebp1* $^{-/-}$ cells treated with thapsigargin. Representative blots are shown in the upper panel; data from four experiments are summarized in the lower panel.

(F) *Chop* mRNA levels in MIN6*WT* and MIN6*Eif4ebp1* $^{-/-}$ cells treated with thapsigargin.

(G) Greater *Chop* translation in MIN6*Eif4ebp1* $^{-/-}$ cells treated with thapsigargin. MIN6*WT* and MIN6*Eif4ebp1* $^{-/-}$ cells treated with vehicle (C) or thapsigargin (Tg) for 12 hr were labeled with [^{35}S]methionine/cysteine. Lysates were either directly subjected to SDS-PAGE or immunoprecipitated with anti-CHOP antibody. Representative autoradiograms are shown in the left panel; data from four experiments are summarized in the right panel.

Error bars represent SEM. *$p < 0.05$, **$p < 0.01$.

4E-BP1-Deficient β Cells Are More Vulnerable to ER Stress

A 4E-BP1-deficient β cell line, MIN6*Eif4ebp1* $^{-/-}$, was established by crossing *Eif4ebp1*$^{-/-}$ mice (Tsukiyama-Kohara et al., 2001) with IT6 mice expressing SV40 large T antigen in β cells (Miyazaki et al., 1990). MIN6 cells with wild-type *Eif4ebp1* alleles, established in parallel, were designated MIN6*WT* cells. MIN6*Eif4ebp1* $^{-/-}$ cells were more vulnerable to ER stress inducers than MIN6*WT* cells (Figure 3A). 4E-BP1 re-expression restored this diminished viability of MIN6*Eif4ebp1*$^{-/-}$ cells to control levels (Figure S3A). The increased susceptibility to ER stress-induced cell death was accompanied by enhanced caspase-3 cleavage (Figure 3B), indicating that the reduced viability of MIN6*Eif4ebp1*$^{-/-}$ cells was due at least in part to increased apoptosis. In addition, DNA fragmentation under ER stress was greater in *Eif4ebp1*$^{-/-}$ islets than in wild-type islets (Figure S3B). These results suggest that 4E-BP1 induction contributes to β cell survival under ER stress.

We then examined the impact of 4E-BP1 deficiency on the integrity of the eIF4F translational initiation complex. Pull-down assays of eIF4E and its binding partners with a cap analog, 7-methyl-GTP, revealed that thapsigargin-induced 4E-BP1 expression resulted in marked increases in the amounts of hypophosphorylated 4E-BP1 α and β forms bound to eIF4E, displacing eIF4G from eIF4E in MIN6*WT* cells (Figure 3C, compare lane 5 with lane 6). The amount of eIF4G bound to eIF4E was reduced to 63% ± 3% ($n = 4$, $p < 0.05$) of that in vehicle-treated MIN6WT cells. In contrast, levels of eIF4G bound to eIF4E were not decreased by thapsigargin in MIN6*Eif4ebp1*$^{-/-}$ cells (Figure 3C, compare lane 7 with lane 8). Thus, eIF4E availability for translational initiation was greater in MIN6*Eif4ebp1*$^{-/-}$ cells than in MIN6*WT* cells under ER stress. Measurement of the global translation rate revealed that recovery from translational suppression by thapsigargin was more rapid in 4E-BP1-deficient cells (Figure 3D).

Translation of newly synthesized mRNA molecules is reportedly much more dependent on eIF4E availability than that of preexisting mRNAs (Novoa and Carrasco, 1999). Expression of CHOP, a mediator of ER stress-induced apoptosis, was thus studied in MIN6*Eif4ebp1* $^{-/-}$ cells since *Chop* mRNA is one of the transcripts most abundantly synthesized during ER stress (Pirot et al., 2007). *Eif4ebp1* deletion caused greater CHOP protein induction by thapsigargin in MIN6 cells (Figure 3E), with unaltered *Chop* mRNA accumulation (Figure 3F). Pulse-labeling experiments demonstrated enhanced CHOP translation (Figure 3G). Thus, CHOP expression during ER stress was augmented via increased translation in 4E-BP1 deficiency.

Eif4ebp1 Deletion Accelerates β Cell Loss in Mouse Diabetes Models

To examine the roles of 4E-BP1 under ER stress in vivo, *Eif4ebp1*$^{-/-}$ mice on the 129S6 background were fed a high-fat diet (HFD), which is thought to produce ER stress in β cells through peripheral insulin resistance (Scheuner et al., 2005). *Eif4ebp1*$^{-/-}$ mice developed glucose intolerance (Figures S4A and S4B), which was associated with blunted insulin secretion (Figure S4C) and reduced pancreatic insulin content (Figure S4D) as compared to HFD-fed wild-type mice. These data suggest that *Eif4ebp1*$^{-/-}$ mice have a β cell defect. However, HFD-fed *Eif4ebp1*$^{-/-}$ mice gained more weight and were more insulin resistant than HFD-fed wild-type mice (Figures S4E and S4F). Therefore, the possibility remains that β cell failure in HFD-fed *Eif4ebp1*$^{-/-}$ mice resulted from greater ER stress rather than from a defect in β cells lacking 4E-BP1.

We next crossed *Eif4ebp1*$^{-/-}$ mice with two genetic models of diabetes in which β cells are under ER stress, *Ins2*$^{WT/C96Y}$ and *Wfs1* $^{-/-}$ mice on the 129S6 background. 4E-BP1 deficiency did not alter body weight (Figures S5A and S5B) or insulin sensitivity (Figures S5C and S5D) but worsened hyperglycemia in *Ins2*$^{WT/C96Y}$ (Figure 4A) and *Wfs1* $^{-/-}$ (Figure 4B) mice. In *Eif4ebp1*$^{-/-}$ *Ins2*$^{WT/C96Y}$ mice, pancreatic insulin content was less than half of that in *Ins2*$^{WT/C96Y}$ mice at 5 weeks of age (Figure 4C), and the majority of islets in *Eif4ebp1*$^{-/-}$ *Ins2*$^{WT/C96Y}$ mice were smaller as compared to those in *Ins2*$^{WT/C96Y}$ mice (Figure 4D). We also observed a 38% decrease in pancreatic insulin content in *Eif4ebp1*$^{-/-}$ *Wfs1*$^{-/-}$ mice as compared to *Wfs1*$^{-/-}$ mice (Figure 4E). Importantly, the insulin-positive area was smaller in pancreatic sections from *Eif4ebp1*$^{-/-}$ *Wfs1*$^{-/-}$ mice than in pancreatic sections from *Wfs1*$^{-/-}$ mice at 27–30 weeks of age (Figure 4F), indicating that ER stress-mediated β cell loss is exacerbated by 4E-BP1 deficiency in vivo.

Global protein synthesis was studied in these mouse islets. A tendency toward decreased protein synthesis was observed in both *Ins2*$^{WT/C96Y}$ (Figure 4G, hatched bar; $p = 0.074$) and *Wfs1*$^{-/-}$ islets (Figure 4H, hatched bar; $p = 0.079$) as compared to wild-type islets. *Eif4ebp1* deletion ablated this regulation and resulted in significantly increased protein synthesis in *Eif4ebp1*$^{-/-}$ *Ins2*$^{WT/C96Y}$ ($p = 0.013$) and *Eif4ebp1*$^{-/-}$ *Wfs1*$^{-/-}$ ($p = 0.045$) islets as compared to that in corresponding single mutants (compared hatched with filled bars in Figures 4G and 4H). These data suggest that accelerated β cell loss under ER stress is due to deregulated translational control.

DISCUSSION

Our results implicate 4E-BP1, identified as a component of the UPR, in β cell survival under ER stress. Important roles of 4E-BPs under various stress conditions have been recently demonstrated in yeast (Ibrahimo et al., 2006) and *Drosophila* (Teleman et al., 2005; Tettweiler et al., 2005). These data suggest that translational suppression by 4E-BPs is an evolutionarily conserved strategy against stress conditions. Although we focused on β cells, ER stress-mediated induction of 4E-BP1 was also observed in the liver and kidneys, suggesting the general importance of the present findings.

Our results suggest that, in addition to translational regulation by eIF2α phosphorylation due to PERK activation, another mode of translational control mediated by 4E-BP1 plays a role in the maintenance of β cell homeostasis under ER stress. Since translational suppression by eIF2α phosphorylation is transient owing to feedback dephosphorylation by GADD34 (Novoa et al., 2001), prolonged translational suppression by 4E-BP1 might be needed in the later stages of the UPR. However, in contrast to PERK, 4E-BP1 deficiency alone does not cause diabetes in mice under normal conditions, suggesting that 4E-BP1 protein is not a key regulator but rather functions with other molecules to maintain β cell homeostasis under ER stress. The preferential role of 4E-BP1 in the later stages of the UPR might be puzzling since expression of

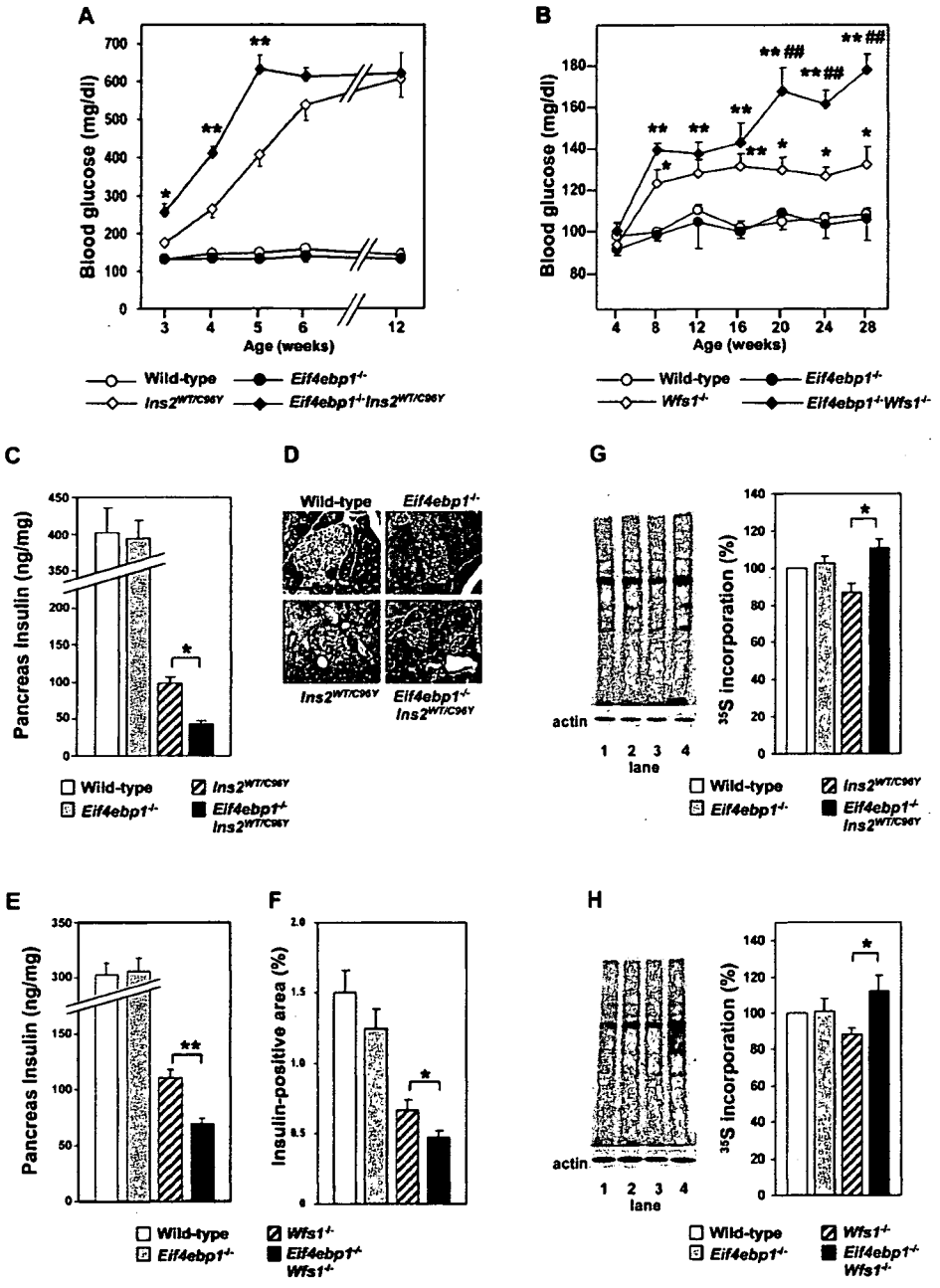

Figure 4. β Cell Loss Is Exacerbated by 4E-BP1 Deficiency in Mouse Diabetes Models

(A) Fed blood glucose levels of wild-type (n = 6), *Eif4ebp1*$^{-/-}$ (n = 5), *Ins2*$^{WT/C96Y}$ (n = 9), and *Eif4ebp1*$^{-/-}$ *Ins2*$^{WT/C96Y}$ (n = 11) mice. Data from three cohorts are combined. *p < 0.05, **p < 0.01 versus *Ins2*$^{WT/C96Y}$ mice.

(B) Fed blood glucose levels of wild-type (n = 12), *Eif4ebp1*$^{-/-}$ (n = 8), *Wfs1*$^{-/-}$ (n = 15), and *Eif4ebp1*$^{-/-}$ *Wfs1*$^{-/-}$ (n = 10) mice. Data from three cohorts are combined. *p < 0.05, **p < 0.01 versus wild-type mice; ##p < 0.01 versus *Wfs1*$^{-/-}$ mice.

(C) Pancreatic insulin content of mice of the indicated genotypes at 5 weeks of age. n = 3 for each genotype. *p < 0.05.

(D) Hematoxylin and eosin staining of sections showing representative islets from mice of the indicated genotypes at 5 weeks of age. Scale bars = 50 μm.

(E) Pancreatic insulin content of wild-type (n = 8), *Eif4ebp1*$^{-/-}$ (n = 4), *Wfs1*$^{-/-}$ (n = 15), and *Eif4ebp1*$^{-/-}$ *Wfs1*$^{-/-}$ (n = 12) mice at 27–30 weeks of age. **p < 0.01.

(F) Insulin-positive area in pancreatic sections of wild-type (n = 3), *Eif4ebp1*$^{-/-}$ (n = 3), *Wfs1*$^{-/-}$ (n = 4), and *Eif4ebp1*$^{-/-}$ *Wfs1*$^{-/-}$ (n = 5) mice at 27–30 weeks of age. *p < 0.05.

(G) [^{35}S]methionine/cysteine incorporation in islets of the indicated genotypes at 5–6 weeks of age. Ten percent of the lysates were also probed with an anti-actin antibody. A representative autoradiogram is shown in the left panel. Lane 1, wild-type; lane 2, *Eif4ebp1*$^{-/-}$; lane 3, *Ins2*$^{WT/C96Y}$; lane 4, *Eif4ebp1*$^{-/-}$ *Ins2*$^{WT/C96Y}$. Data from four experiments are summarized in the right panel. *p < 0.05.